Probing the first order electroweak phase transition by measuring gravitational waves in scalar extension models

Toshinori Matsui

KIAS

KOREA INSTITUTE FOR ADVANCED STUDY

Collaborators: Katsuya Hashino[1], Mitsuru Kakizaki[1], Shinya Kanemura[2], Pyungwon Ko[3]

[1]University of TOYAMA, [2]Osaka University, [3]KIAS

K. Hashino, M. Kakizaki, S. Kanemura, TM, P. Ko, Phys. Lett. B **766**, 49 (2017) [arXiv:1609.00297]

Motivation

- Discovery of the Higgs boson
  - Mass generation mechanism is confirmed
  - The standard model as an effective theory is established
- What is the nature of electroweak symmetry breaking?
  - SM have minimal Higgs potential…**no principle**
  - Higgs self-couplings **have not been measured**

    →We have not understood the shape of the Higgs potential

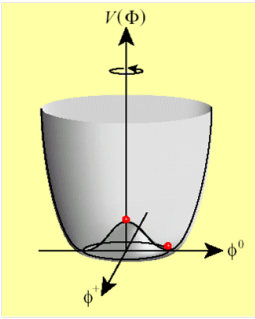

- Exploring the structure of the Higgs sector is important
  - New physics is required to solve BSM phenomena

    Baryon asymmetry of the Universe, Existence of dark matter,…
  - BSM might be related to the extended Higgs sector

    EW baryogenesis, Radiative neutrino mass models, …

Electroweak Baryogenesis

~ Importance to understand the Higgs potential ~

- Observed Baryon number: $n_B/s \simeq \mathcal{O}(10^{-10})$
- Sakharov's three conditions

  1. #B violation, 2. CP violation, 3. Departure from equilibrium

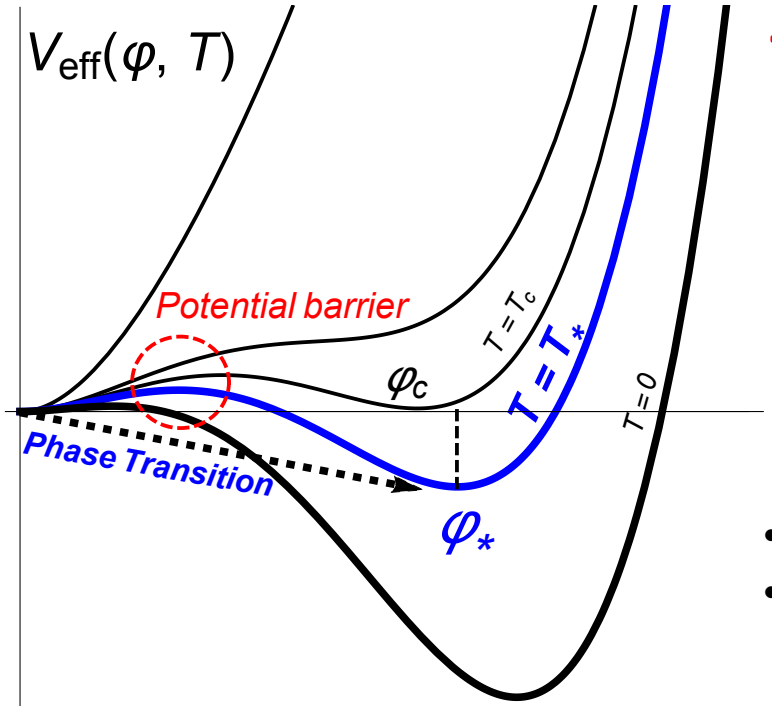

→Strongly 1st order phase transition

$$\varphi_*/T_* \gtrsim 1$$

- SM (m_h=125GeV) cannot satisfy these conditions.
- Strongly 1stOPT is realized by models with extended Higgs sector.

Strongly 1stOPT and Higgs boson couplings

~ Probing the Higgs potential by "future colliders" ~

- Potential barrier can be created by thermal loop effects

The strength of phase transition (analytic formula for one field by high temperature approximation)

$$\varphi_c/T_c = 2E/\lambda(T_c) \gtrsim 1 \qquad V_{\rm eff} = D(T^2 - T_0^2)\varphi^2 - ET\varphi^3 + \frac{\lambda(T)}{4}\varphi^4$$

e.g. Two Higgs doublet model (2HDM)

$$m_\Phi^2 \simeq M^2 + \lambda_i v^2 \quad \Phi = H, A, H^\pm$$

$$E = \frac{1}{12\pi v^3}\left\{6m_{W^\pm}^3 + 3m_Z^3 + \sum_\Phi m_\Phi^3\left(1 - \frac{M^2}{m_\Phi^2}\right)^3\left(1 + \frac{3}{2}\frac{M^2}{m_\Phi^2}\right)\right\}$$

Enhanced by $M \to 0$ limit (large λ_i)

Strongly 1st OPT and Higgs boson couplings

~ Probing the Higgs potential by "future colliders" ~

- Potential barrier can be created by thermal loop effects

The strength of phase transition (analytic formula for one field by high temperature approximation)

$$\varphi_c/T_c = 2E/\lambda(T_c) \gtrsim 1 \qquad V_{\rm eff} = D(T^2 - T_0^2)\varphi^2 - ET\varphi^3 + \frac{\lambda(T)}{4}\varphi^4$$

e.g. Two Higgs doublet model (2HDM)

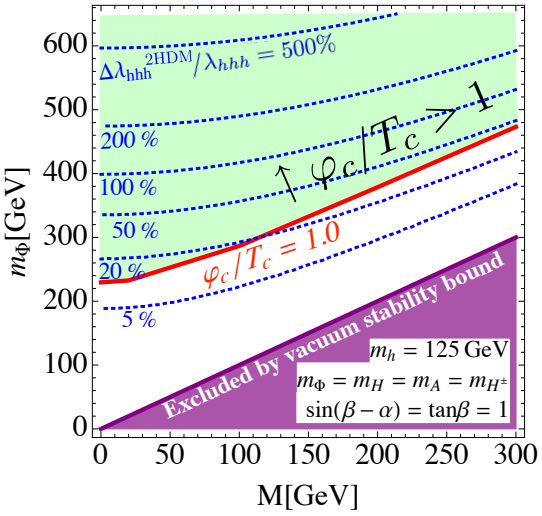

$$m_\Phi^2 \simeq M^2 + \lambda_i v^2 \qquad \Phi = H, A, H^\pm$$

$$E = \frac{1}{12\pi v^3}\left\{6m_{W^\pm}^3 + 3m_Z^3 + \sum_\Phi m_\Phi^3\left(1 - \frac{M^2}{m_\Phi^2}\right)^3\left(1 + \frac{3}{2}\frac{M^2}{m_\Phi^2}\right)\right\}$$

$$\frac{\Delta\lambda_{hhh}}{\lambda_{hhh}} \equiv \frac{\lambda_{hhh} - \lambda_{hhh}^{\rm SM}}{\lambda_{hhh}^{\rm SM}}$$

Enhanced by $M \to 0$ limit (large λ_i)

$$\lambda_{hhh}^{\rm 2HDM} \equiv \frac{3m_h^2}{v}\left\{1 - \frac{m_t^4}{\pi^2 m_h^2 v^2} + \sum_\Phi \frac{m_\Phi^4}{12\pi^2 m_h^2 v^2}\left(1 - \frac{M^2}{m_\Phi^2}\right)\right\}$$

Kanemura, Okada, Senaha, PLB**606**, 361 (2005)

Large deviation in the *hhh* coupling is required! → EWPT can be tested at future colliders!

Gravitational waves

~ Probing the Higgs potential by "future GW observations" ~

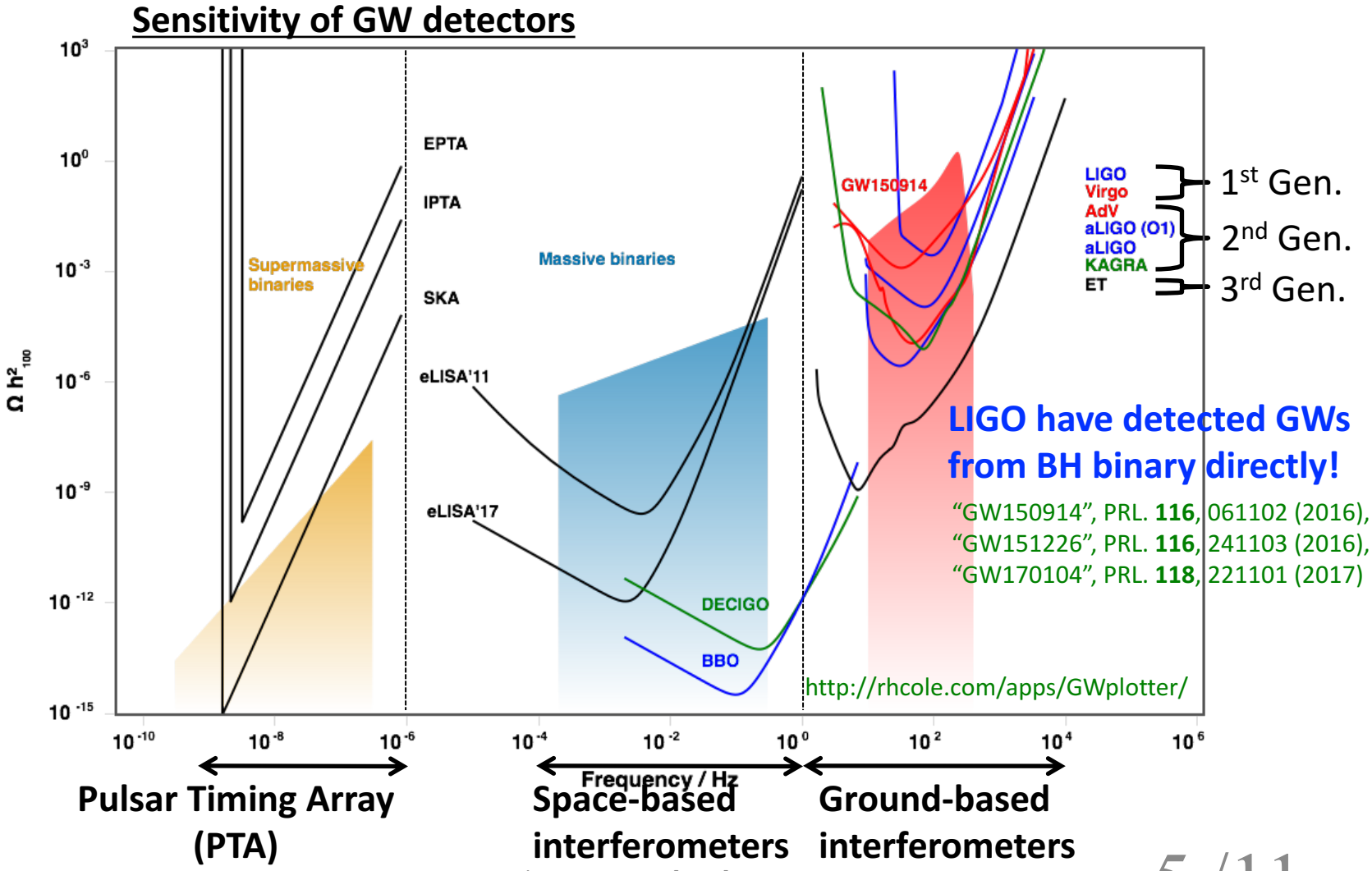

Gravitational waves

~ Probing the Higgs potential by "future GW observations" ~

Red shifted frequency:

$$f_0 = \frac{a_t}{a_0} f_t$$

EWPT (~100GeV)

$$f_0 \simeq 10^{-5}\mathrm{Hz}\frac{T_t}{100\mathrm{GeV}}\frac{f_t}{H_t}$$

$$(f_t \simeq 10^9 \mathrm{Hz})$$

EWPT can be explored at future space-based interferometers!

Sensitivity of GW detectors

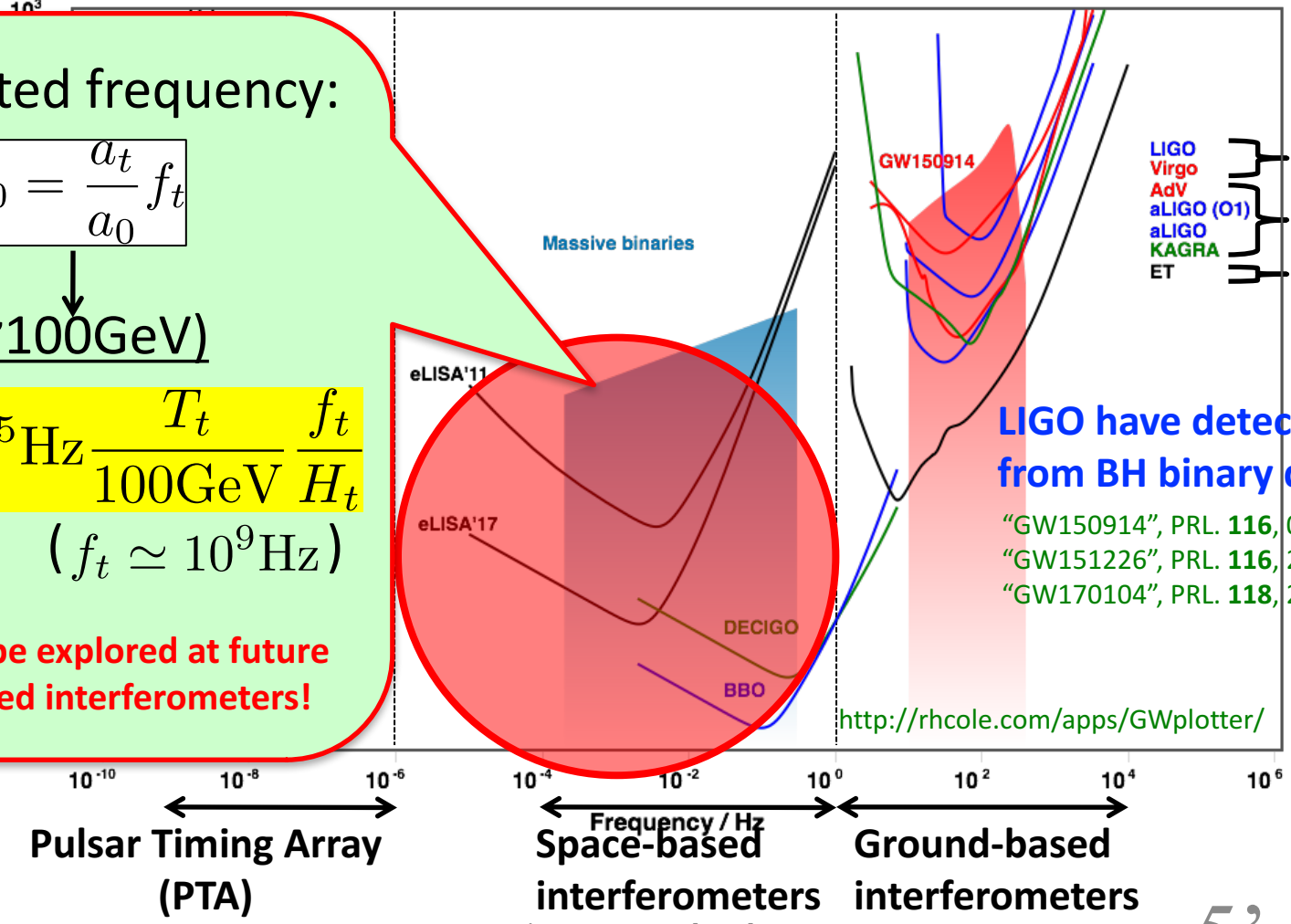

LIGO have detected GWs from BH binary directly!

"GW150914", PRL. **116**, 061102 (2016),
"GW151226", PRL. **116**, 241103 (2016),
"GW170104", PRL. **118**, 221101 (2017)

Pulsar Timing Array (PTA) | **Space-based interferometers** | **Ground-based interferometers**

GWs from 1stOPT

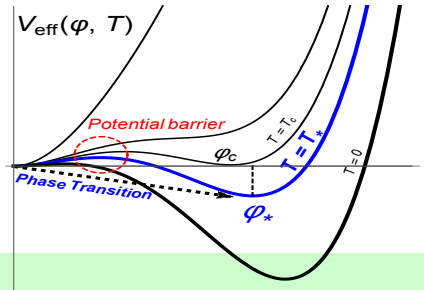

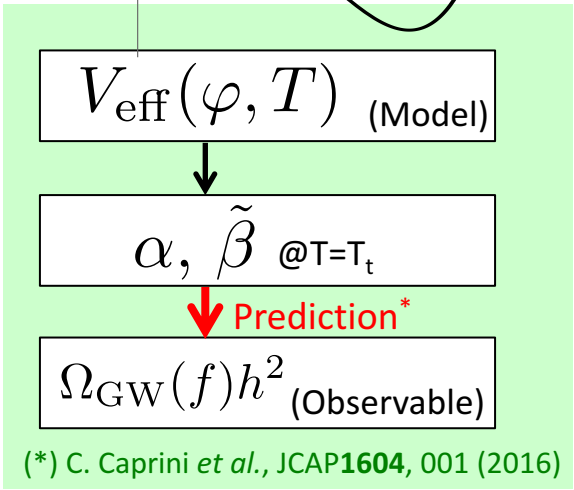

(*) C. Caprini *et al.*, JCAP**1604**, 001 (2016)

Characteristic parameters of 1stOPT

"Normalized difference of the potential minima"

- α is defined as $\alpha \equiv \left.\dfrac{\epsilon}{\rho_{\rm rad}}\right|_{T=T_t}$. ($\rho_{\rm rad}$ is energy density of rad.)
  - Latent heat: $\epsilon(T) \equiv -\Delta V_{\rm eff}(\varphi_B(T), T) + T\dfrac{\partial \Delta V_{\rm eff}(\varphi_B(T))}{\partial T}$

"~How fast the minimum goes down"

- β is defined as $\beta \equiv \left.\dfrac{1}{\Gamma}\dfrac{d\Gamma}{dt}\right|_{t=t_t}$. → $\tilde{\beta}\left(\equiv \dfrac{\beta}{H_t}\right) = T_t \left.\dfrac{d(S_3(T)/T)}{dT}\right|_{T=T_t}$
  - Bubble nucleation rate: $\Gamma(T) \simeq T^4 e^{-\frac{S_3(T)}{T}}$
  - 3-dim. Euclidean action: $S_3(T) = \int dr^3 \left\{\dfrac{1}{2}\left(\vec{\nabla}\varphi\right)^2 + V_{\rm eff}(\varphi, T)\right\}$

Three sources of GWs (relic abundance @ peak frequency)

"Sound waves" (Compressional plasma)
"Bubble collision" (Envelope approximation)
"Magnetohydrodynamic turbulence in the plasma"

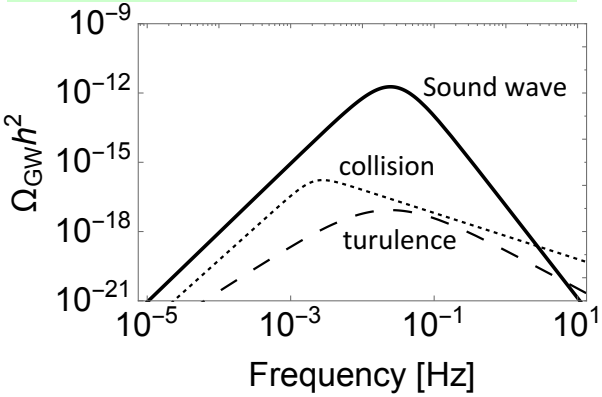

Models of 1stOPT

Higgs potential by high temperature approximation

$$V_{\rm eff} = D(T^2 - T_0^2)\varphi^2 - (ET - e)\varphi^3 + \frac{\lambda(T)}{4}\varphi^4 \Rightarrow \frac{\varphi_c}{T_c} = \frac{2E}{\lambda}\left(1 - \frac{e\lambda}{ET}\right)$$

- E : thermal coupling (the non-decoupling effects due to the additional boson loop)
- $-e$: non-thermal coupling (the field mixing of the Higgs boson with additional scalar fields)

Models of 1stOPT

Higgs potential by high temperature approximation

$$V_{\rm eff} = D(T^2 - T_0^2)\varphi^2 - (ET - e)\varphi^3 + \frac{\lambda(T)}{4}\varphi^4$$

$$\frac{\varphi_c}{T_c} = \frac{2E}{\lambda}\left(1 - \frac{e\lambda}{ET}\right)$$

- E : thermal coupling (the non-decoupling effects due to the additional boson loop)
- $-e$: non-thermal coupling (the field mixing of the Higgs boson with additional scalar fields)

J. Kehayias and S. Profumo, JCAP**1003**, 003 (2010)

$$115\text{GeV} \le m_h < 348\text{GeV}$$

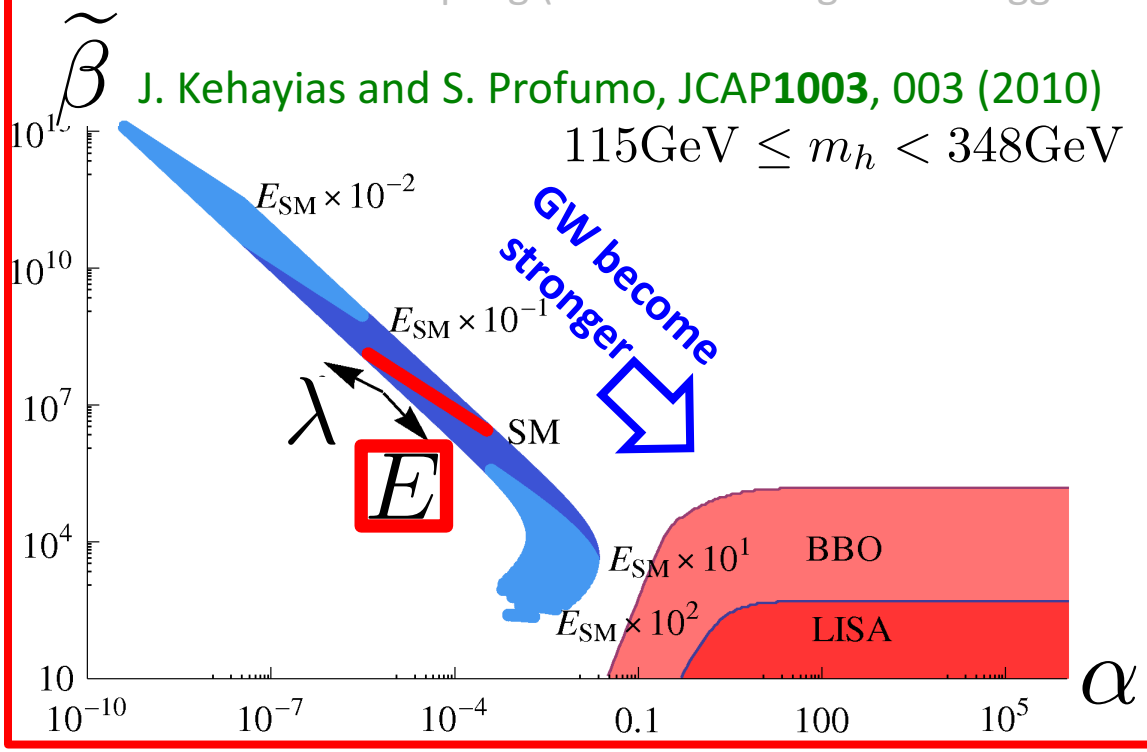

As the simplest model, we have investigated **the O(N) model**.

Kakizaki, Kanemura, TM, PRD **92**, 115007 (2015);
Hashino, Kakizaki, Kanemura, TM, PRD **94**, 015005 (2016)

Models of 1stOPT

Higgs potential by high temperature approximation

$$V_{\rm eff} = D(T^2 - T_0^2)\varphi^2 - (ET - e)\varphi^3 + \frac{\lambda(T)}{4}\varphi^4$$

$$\frac{\varphi_c}{T_c} = \frac{2E}{\lambda}\left(1 - \frac{e\lambda}{ET}\right)$$

- E : thermal coupling (the non-decoupling effects due to the additional boson loop)
- $-e$: non-thermal coupling (the field mixing of the Higgs boson with additional scalar fields)

$\widetilde{\beta}$

J. Kehayias and S. Profumo, JCAP**1003**, 003 (2010)

$$115\text{GeV} \le m_h < 348\text{GeV}$$

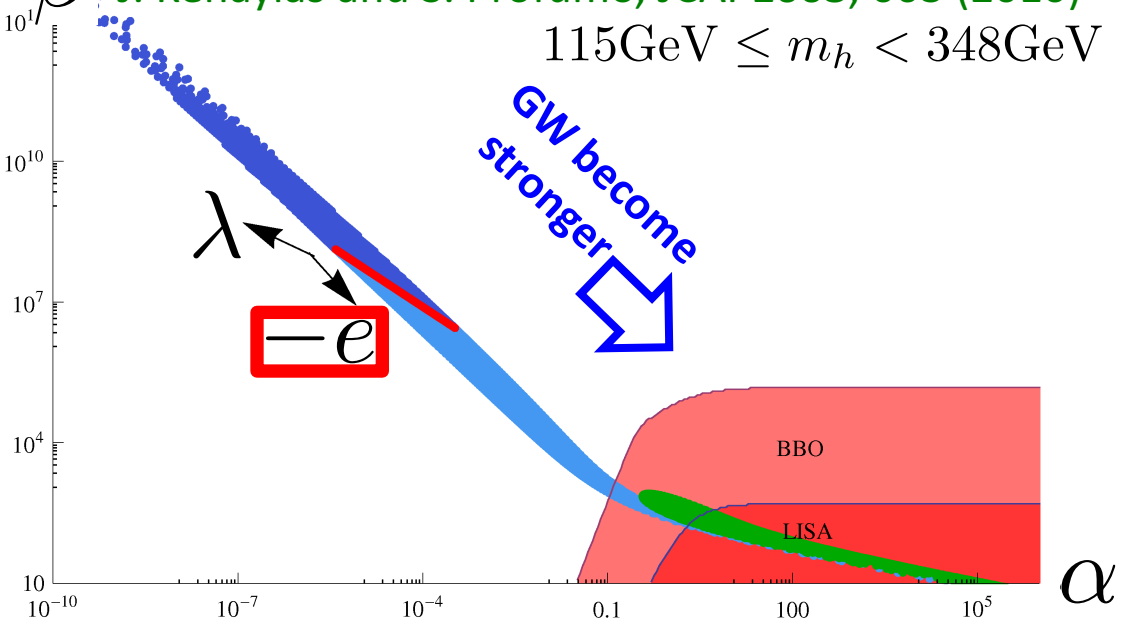

As the simplest model,
we have investigated
the Higgs singlet model.

Hashino, Kakizaki, Kanemura, TM, Ko,
PLB **766**, 49 (2017)

Higgs singlet model

Fuyuto, Senaha, PRD **90**, 015015 (2014),
Hashino, Kakizaki, Kanemura, TM, Ko, PLB **766**, 49 (2017),…

- Higgs potential (8 parameters) $\Phi = \begin{pmatrix} G^+ \\ \frac{1}{\sqrt{2}}(v_\Phi + \phi_1 + iG^0) \end{pmatrix}, \quad S = v_S + \phi_2$

$$V_0 = -\mu_\Phi^2|\Phi|^2 + \lambda_\Phi|\Phi|^4 + \mu_{\Phi S}|\Phi|^2 S + \frac{\lambda_{\Phi S}}{2}|\Phi|^2 S^2 + \mu_S^3 S + \frac{m_S^2}{2}S^2 + \frac{\mu_S'}{3}S^3 + \frac{\lambda_S}{4}S^4$$

  - Tadpole conditions → (v_Φ, v_S)
  - Diagonalized mass matrix in (ϕ_1, ϕ_2)→(m_h, m_H) and θ

- Two-field analysis @finite *T*

Diverse patterns of phase transition →

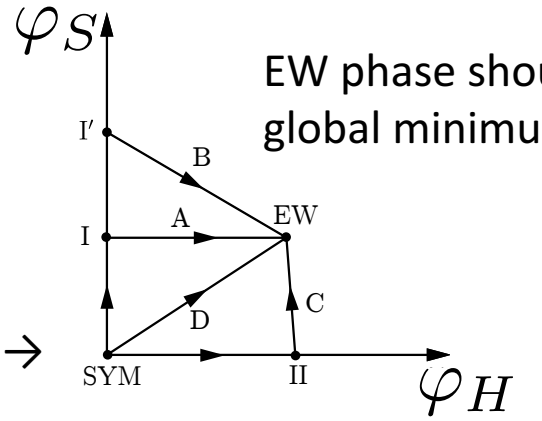

EW phase should be global minimum at *T*=0.

Collider experiments

- Higgs couplings: $\kappa \equiv \kappa_V = \kappa_F = \cos\theta$ $\kappa_i \equiv g_{hii}/g_{hii}^{\rm SM}$
  - recent LHC data: $\kappa_Z = 1.03^{+0.11}_{-0.11}, \kappa_W = 0.91^{+0.10}_{-0.10}$
    (1σ; combination of ATLAS and CMS) [ATLAS-CONF-2015-044]
  - Expected accuracy: 2%@HL-LHC 14TeV 3000fb^{-1} [CMS collaboration, 1307.7135],
    0.37% (0.51%) for κ_Z (κ_W)@ILC 500GeV 500fb^{-1} [Fujii et al, 1506.05992]
- Deviation of *hhh* coupling from SM: $\Delta\lambda_{hhh} \equiv \frac{\lambda_{hhh}^{\rm HSM} - \lambda_{hhh}^{\rm SM}}{\lambda_{hhh}^{\rm SM}}$
  - Expected accuracy: 54%@HL-LHC 14TeV 3000fb^{-1} [CMS-PAS-FTR-15-002],
    27%@ILC 500GeV 4000fb^{-1} [Fujii et al, 1506.05992],
    16% (10%)@ILC 1TeV 2000fb^{-1} (5000fb^{-1}) [Fujii et al, 1506.05992]

Numerical results

- Benchmark point:

v_Φ [GeV]	v_S [GeV]	m_h [GeV]	$\mu_{\Phi S}$ [GeV]	μ'_S [GeV]	μ_S [GeV]	m_H [GeV]	θ [degrees]
246.2	90	125.5	-80	-30	0	[160, 240]	[-15, -35]

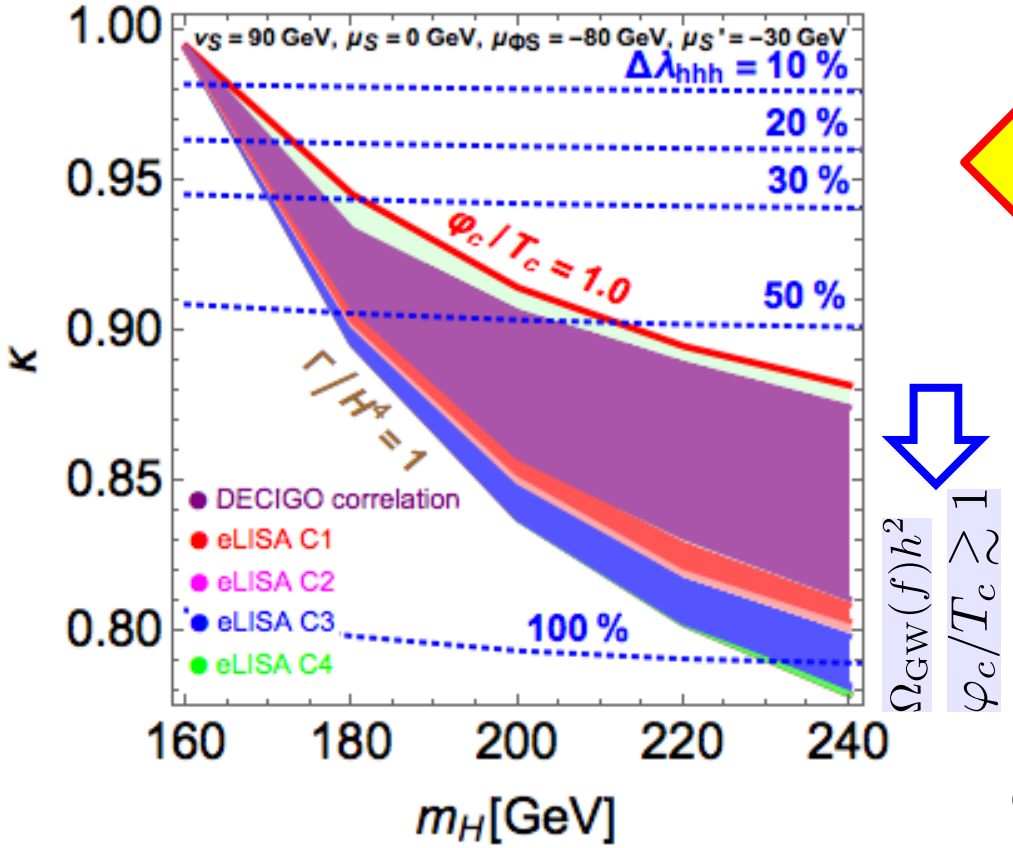

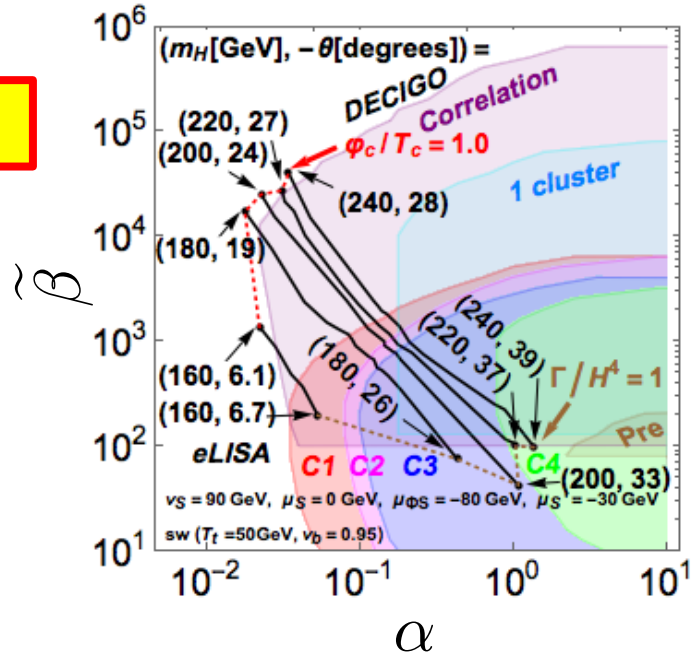

DECIGO [Class. Quant. Grav. 28, 094011 (2011)],
eLISA [arXiv:1512.06239]

Hashino, Kakizaki, Kanemura, TM, Ko, PLB **766**, 49 (2017)

Numerical results

The synergy between the precision measurements of the Higgs boson couplings and GWs at future experiments is important!

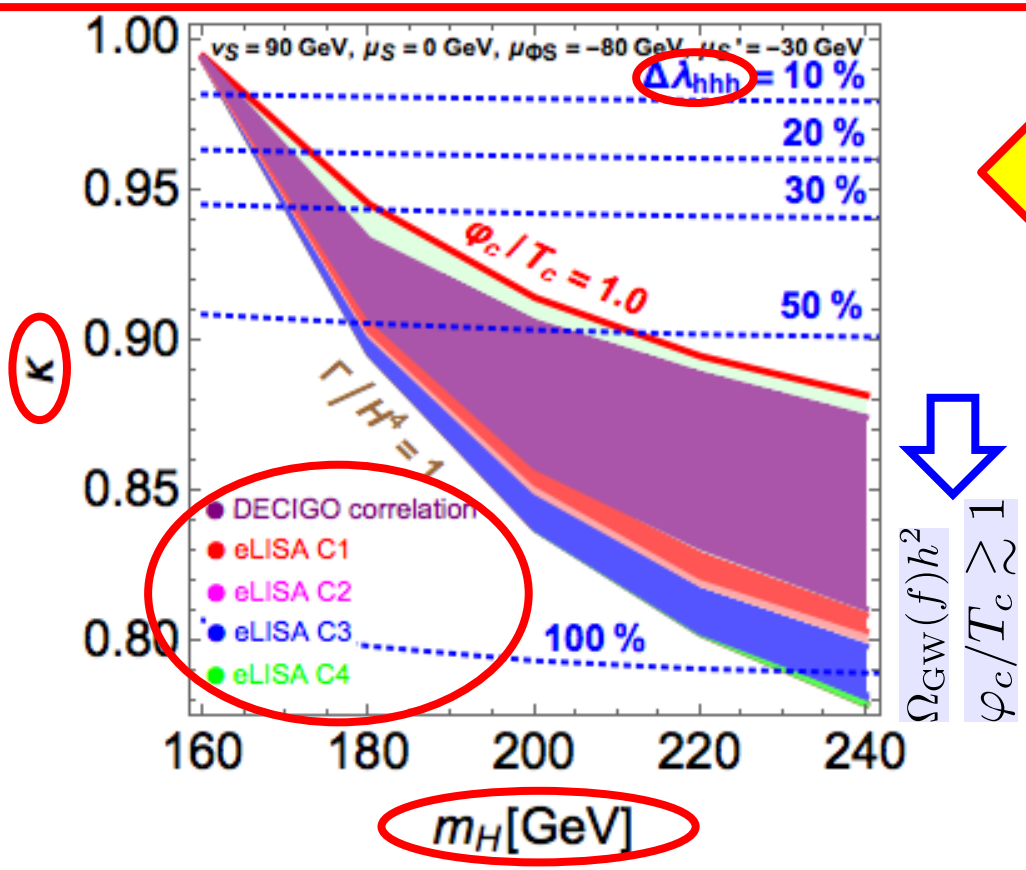

$\Omega_{GW}(f)h^2$

$\varphi_c/T_c \gtrsim 1$

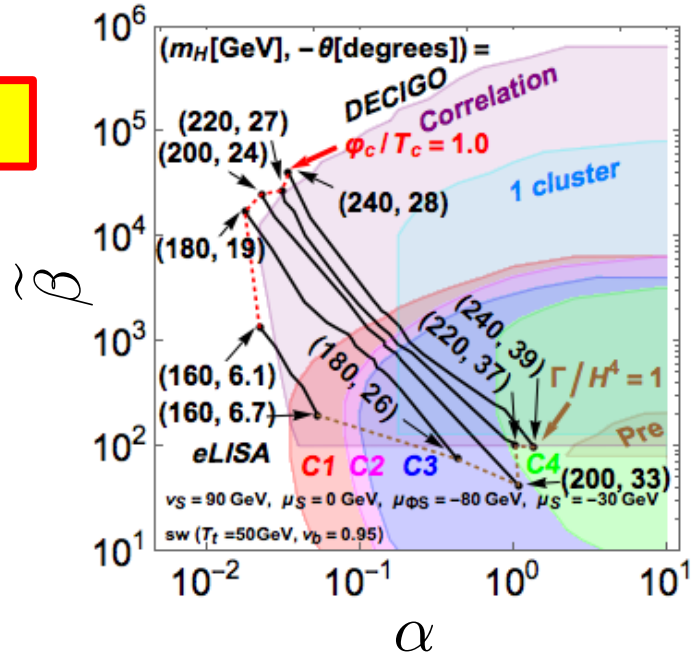

DECIGO [Class. Quant. Grav. 28, 094011 (2011)],
eLISA [arXiv:1512.06239]

Hashino, Kakizaki, Kanemura, TM, Ko, PLB **766**, 49 (2017)

Conclusions

- Exploring the structure of the Higgs sector is important to understand physics behind EWSB.
- We have investigated various models of 1stOPT.
- The strongly 1stOPT of EWSB can be tested by the measurements of various Higgs boson couplings @LHC, the *hhh* coupling @ILC and GWs @future space-based interferometers.

Back Up

Gravitational wave observations

Gravitational waves

～ Probing the Higgs potential by GW observations ～

LIGO have detected GWs directly.

"GW150914", PRL. **116**, 061102 (2016),
"GW151226", PRL. **116**, 241103 (2016),
"GW170104", PRL. **118**, 221101 (2017)

- Ground exp.: aLIGO [USA], KAGRA [JPN], aVIRGO [ITA･FRA],…
  → Just now observing GWs directly from astronomical phenomena such as the binary of black holes, neutron stars, etc.

The era of GW astronomy will come true!

- Future space exp.: eLISA [EU], DECIGO [JPN], BBO [USA]…
  → Will be exploring phenomena at the early stage of the Universe such as EW phase transition (EWPT), cosmic inflation, topological defects, etc.

We expect GWs as a new technique to explore the BSM, in addition to the collider experiments!

Experimental status (eLISA)

- LISA pathfinder: launched on Dec., 2015, reported results [PRL**116**, 231101 (2016)]
- **eLISA design with 3 arms was decided**. http://www.physik.uzh.ch/events/lisa2016
- ESA approval: June, 2017 → eLISA launch : **2034**

LIGO have detected GWs

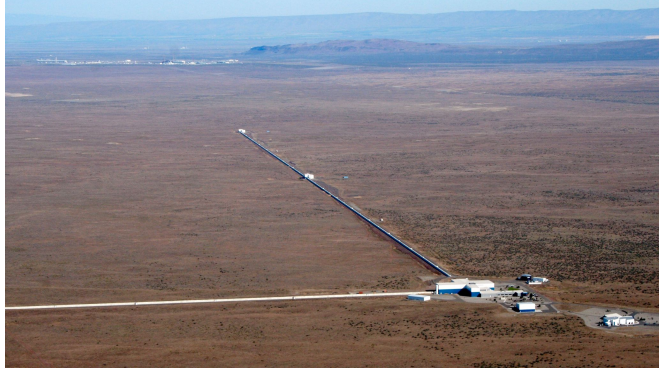

- “GW150914” LIGO Scientific and Virgo Collaborations, Phys. Rev. Lett. **116**, no. 6, 061102 (2016)
  - BH merger (36+29→62 in the unit of solar mass)
  - 410Mpc (1.3 billion years ago)
  - Signal/Noise=24 (>5.1σ), frequency: 35-250 Hz
- "GW151226” LIGO Scientific and Virgo Collaborations, Phys. Rev. Lett. **116**, no. 24, 241103 (2016)
  - BH merger (14+8→21 in the unit of solar mass)
  - 440Mpc (1.4 billion years ago)
  - Signal/Noise=13 (>5σ), frequency: 35-450 Hz,

Prospects for LIGO/Virgo

- LIGO 1st RUN (2015/09/12-2016/01/19)
- LIGO 2nd RUN (from the fall 2016)
  - 15-25% improvement in sensitivity performance over 1st RUN
  - The event rate will be increased by 1.5-2 times

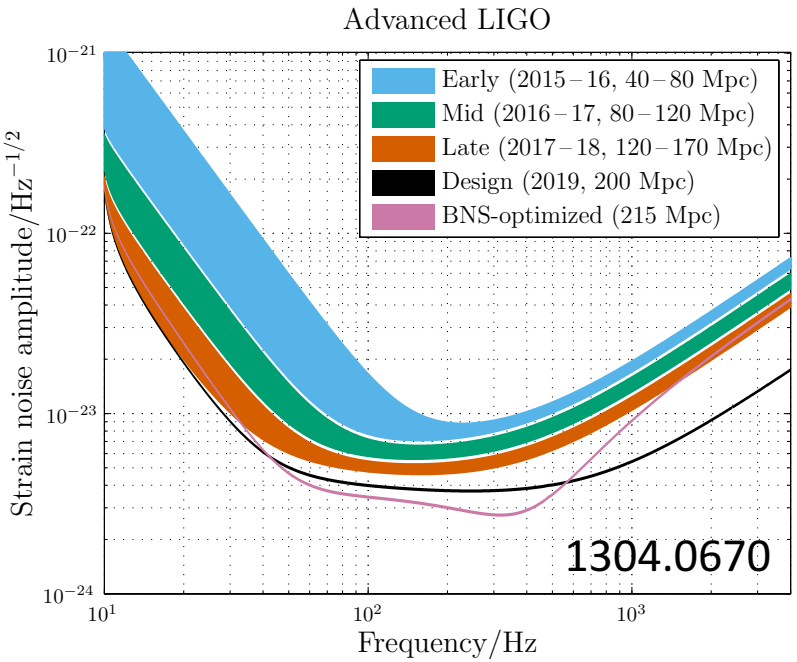

Observing run	Epoch	Duration (months)	aLIGO sensitivity	AdVirgo sensitivity
O1	2015–2016	4	Early	—
O2	2016–2017	6	Mid	Early
O3	2017–2018	9	Late	Mid
O4	2019	12	Design	Late
O5	2020+	–	Design	Design

1602.03847

Pulsar Timing Array

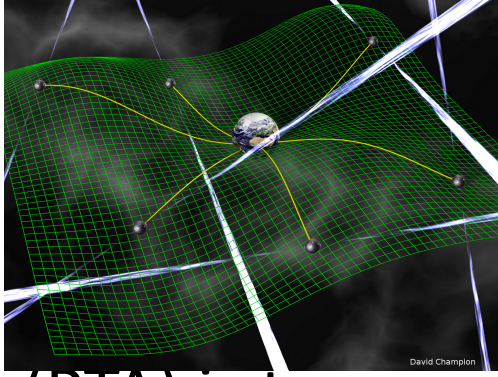

- The main idea behind pulsar timing array (PTA) is to use ultra-stable millisecond pulsars as beacons for detecting GW in the nano-Hz range (10^{-9} – 10^{-7} Hz).
- Pulsars are neutron stars with rapid rotation and strong magnetic field. Period from few seconds to few milliseconds.

Pulsar Timing Array

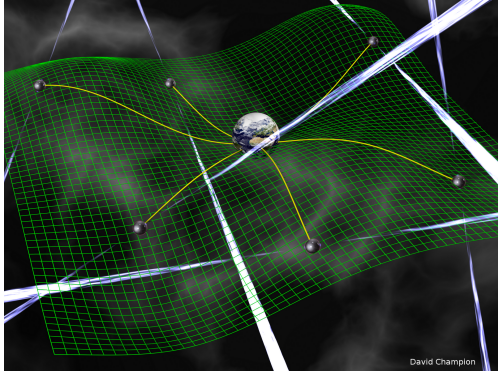

- Current limit: $\Omega_{GW}h^2>\sim10^{-9}$

  EPTA Collaboration [Mon. Not. Roy. Astron. Soc. **453**, no. 3, 2576 (2015) [arXiv:1504.03692]]

  NANOGrav Collaboration [Astrophys. J. **821**, no. 1, 13 (2016) [arXiv:1508.03024]]

- **International Pulsar Timing Array** (IPTA): combined three PTAs [PPTA (Australian), EPTA (European)*, NanoGrav (North American)]. *EPTA consists of 5 radio telescopes

  1st data release Mon. Not. Roy. Astron. Soc. **458**, 1267 (2016) [arXiv:1602.03640]

  Expected limit: $\Omega_{GW}h^2>\sim10^{-12}$ Publ. Astron. Soc. Austral. **30**, 17 (2013) [arXiv:1210.6130]

- **Square Kilometer Array** (SKA)

  : The next great advancement in radio astronomy

  Expected limit: $\Omega_{GW}h^2>\sim10^{-15}$ https://www.skatelescope.org

Properties of the representative eLISA configurations

eLISA cosmology WG report, JCAP**1604**, 001 (2016) [arXiv:1512.06239]

- **Number of laser links :** 4 or 6, corresponding to 2 or 3 interferometer arms

- **Arm length :** 1 / 2 / 5 million km
- **Duration :** 2 / 5 years data taking
- **Noise level** : N2 (LISA pathfinder expected) is 10 times larger than N1 (LISA pathfinder required)

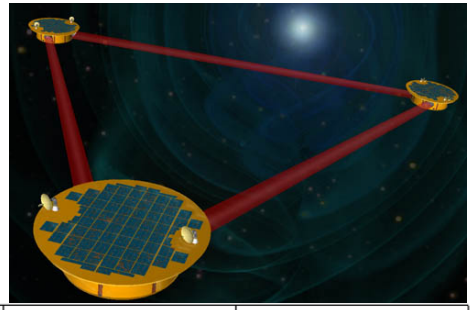

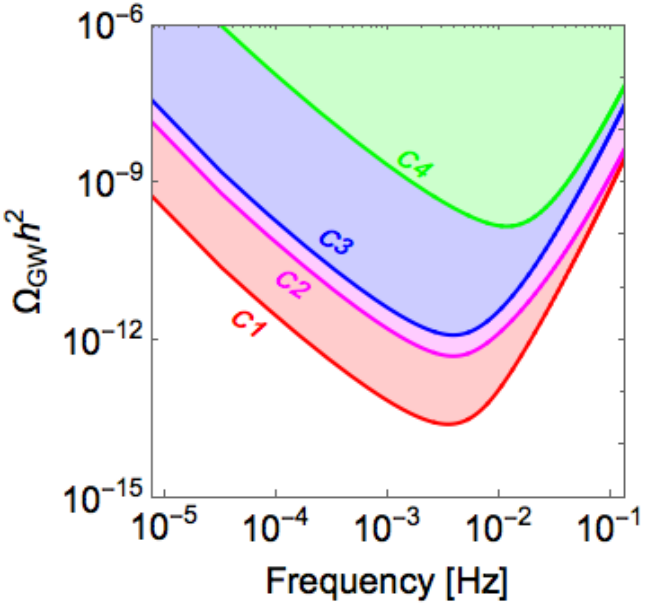

Name	C1	C2	C3	C4
Full name	N2A5M5L6	N2A1M5L6	N2A2M5L4	N1A1M2L4
# links	6	6	4	4
Arm length [km]	5M	1M	2M	1M
Duration [years]	5	5	5	2
Noise level	N2	N2	N2	N1

eLISA design decided

Extra budget (partially because of re-analyses of costs, partially because of NASA+Japan)

- **Number of laser links :** ~~4 or~~ **6**, corresponding to ~~2 or~~ **3** interferometer arms
  → Determined at eLISA symposium (Sept. 2016, U. of Zurich) http://www.physik.uzh.ch/events/lisa2016
- **Arm length :** ~~1 / 2 / 5~~ **2 - 5** million km
- **Duration :** ~~2 / 5~~ **3 - 10** years data taking
- **Noise level** : **N2** (LISA pathfinder expected) is 10 times larger than ~~N1 (LISA pathfinder required)~~
  → Determined by receiving the pathfinder result [PRL**116**, 231101 (2016)]

launch : **2034**

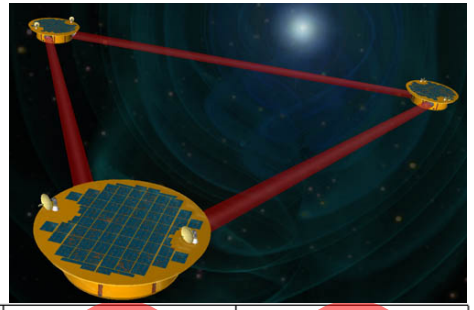

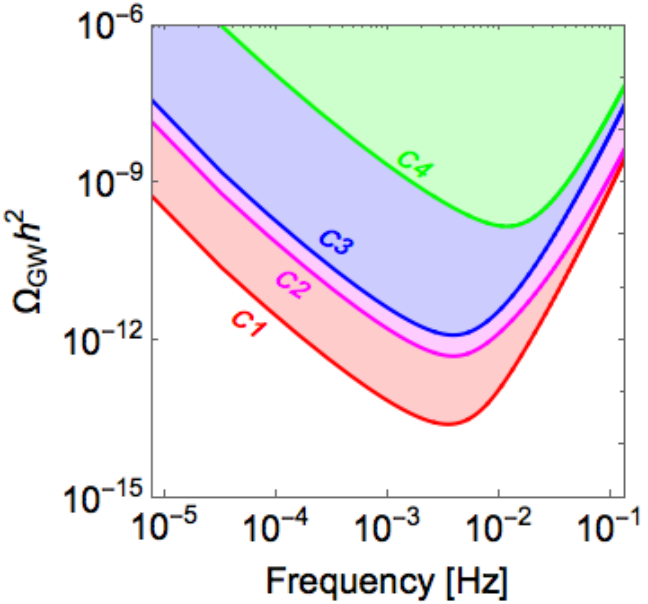

Name	C1	C2	C3	C4
Full name	N2A5M5L6	N2A1M5L6	N2A2M5L4	N1A1M2L4
# links	6	6	4	4
Arm length [km]	5M	1M	2M	1M
Duration [years]	5	5	5	2
Noise level	N2	N2	N2	N1

C1 corresponds to the old LISA configuration

Gravitational wave from 1st order phase transition

Phase transition - Bubble configuration

Model parameters

Input

$V_{\rm eff}(\varphi, T)$ → $\Gamma(T)$

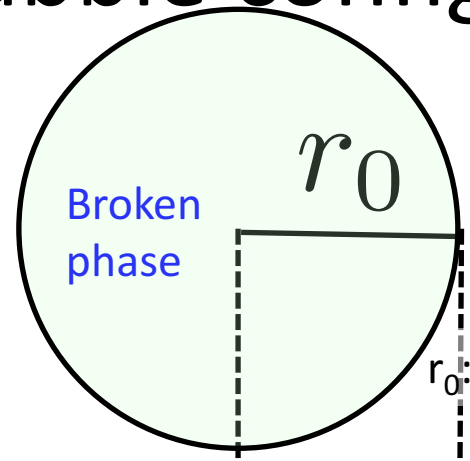

r_0: size of critical bubble

Potential:

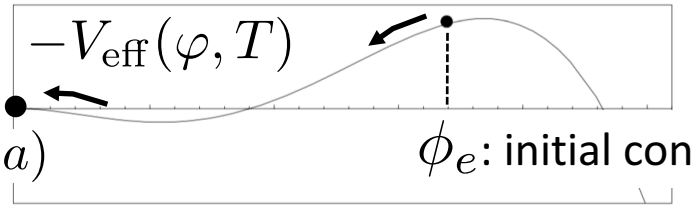

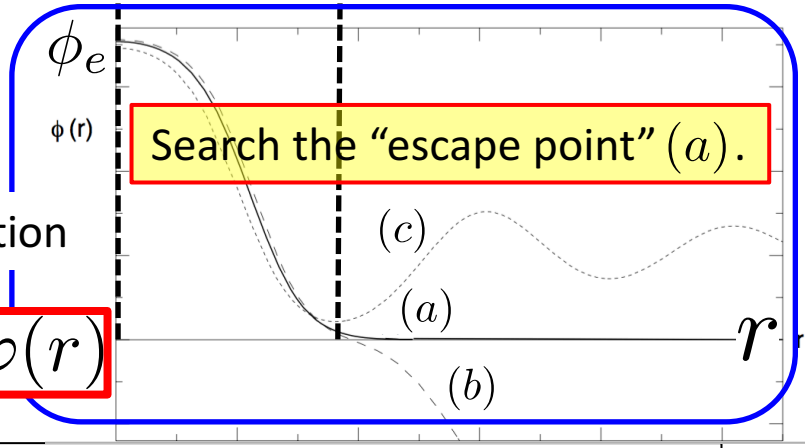

Eq. of motion: $\frac{d^2\varphi}{dr^2} + \frac{2}{r}\frac{d\varphi}{dr} - \frac{dV_{\rm eff}}{d\varphi} = 0$ → $\varphi(r)$

$\varphi(r)$ → each T

Bubble nucleation rate: $\Gamma(T) \simeq T^4 e^{-\frac{S_3(T)}{T}}$

3-dim. Euclidean action: $S_3(T) = \int dr^3 \left\{ \frac{1}{2}\left(\vec{\nabla}\varphi\right)^2 + V_{\rm eff}(\varphi, T) \right\}$

Phase transition - Transition temperature

Model parameters

Input

$V_{\rm eff}(\varphi, T)$ → $\Gamma(T)$

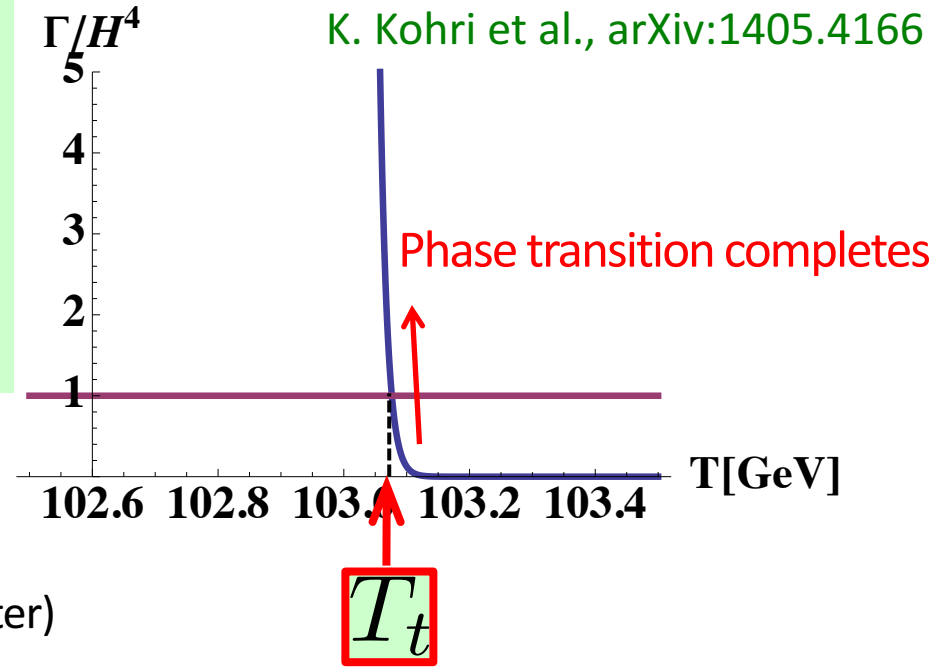

K. Kohri et al., arXiv:1405.4166

Phase transition completes

$$\left.\frac{\Gamma}{H^4}\right|_{T=T_t} \simeq 1$$

(*H*: Hubble parameter)

→Definition of phase transition temperature T_t

Bubble nucleation rate: $\Gamma(T) \simeq T^4 e^{-\frac{S_3(T)}{T}}$

3-dim. Euclidean action: $S_3(T) = \int dr^3 \left\{ \frac{1}{2} \left(\vec{\nabla}\varphi \right)^2 + V_{\rm eff}(\varphi, T) \right\}$

GWs from 1stOPT

Model parameters

Input

$V_{\rm eff}(\varphi, T)$ → $S_3(T)$

Definition of phase transition temperature T_t

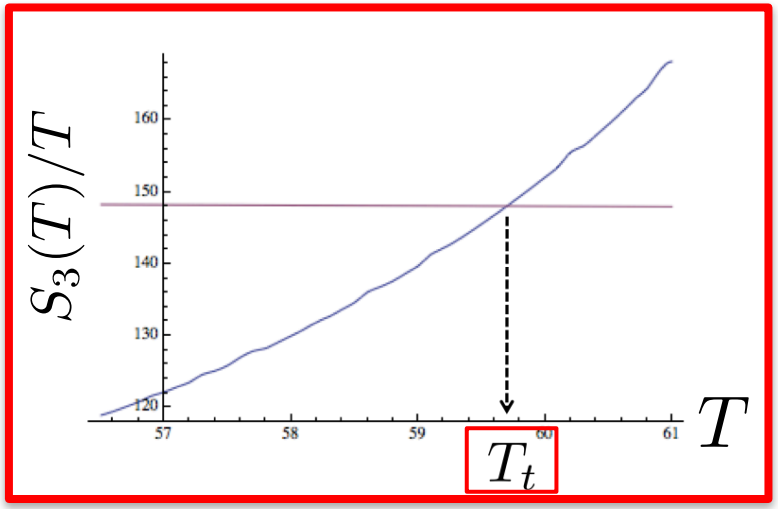

$$\left.\frac{\Gamma}{H^4}\right|_{T=T_t} \simeq 1 \quad \Leftrightarrow \quad \left.\frac{S_3(T)}{T}\right|_{T=T_t} \simeq 140-150$$

$$\Gamma(T) \simeq T^4 e^{-\frac{S_3(T)}{T}}$$

$$S_3(T) = \int dr^3 \left\{ \frac{1}{2}\left(\vec{\nabla}\varphi\right)^2 + V_{\rm eff}(\varphi, T) \right\}$$

Behavior of S_3/T↑

GWs from 1stOPT

Model parameters

Input

$V_{\rm eff}(\varphi, T)$ → $S_3(T)$

Definition of phase transition temperature T_t

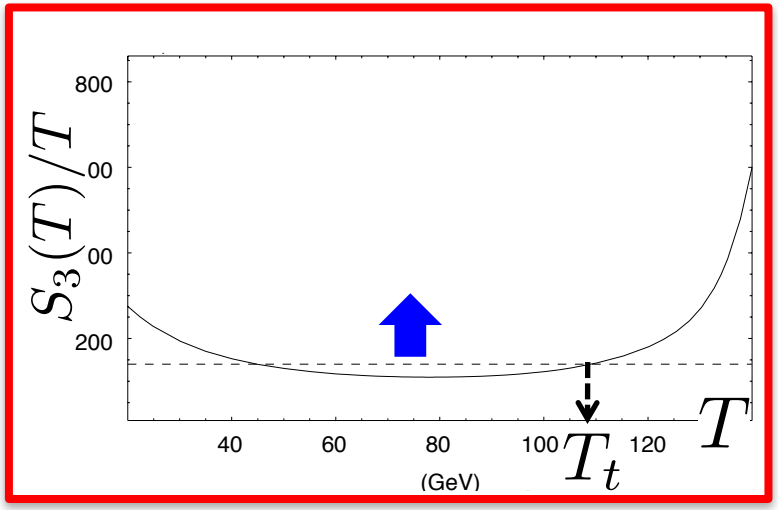

$$\left.\frac{\Gamma}{H^4}\right|_{T=T_t} \simeq 1 \quad \Leftrightarrow \quad \left.\frac{S_3(T)}{T}\right|_{T=T_t} \simeq 140 - 150$$

Model parameters are constrained.

R. Apreda et al., NPB**631**, 342 (2002)

Behavior of S_3/T↑

Phase transition - Characteristic parameters

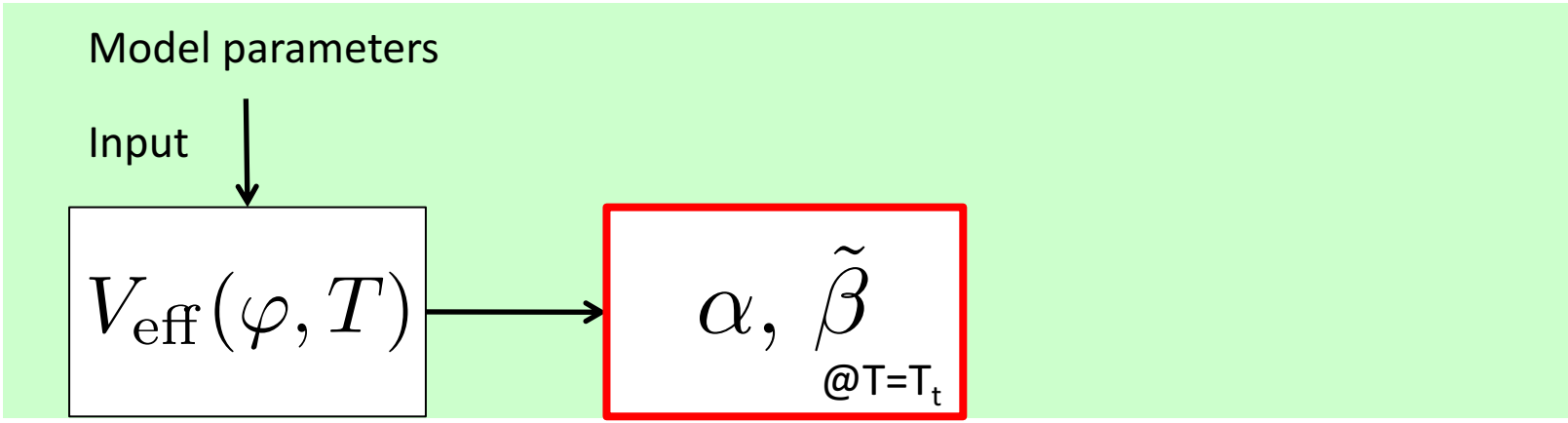

- α is defined as $\alpha \equiv \left.\frac{\epsilon}{\rho_{\rm rad}}\right|_{T=T_t}$ is energy density of rad.)
  - Latent heat: $\epsilon(T) \equiv -\Delta V_{\rm eff}(\varphi_B(T), T) + T\frac{\partial \Delta V_{\rm eff}(\varphi_B(T))}{\partial T}$ cf. U=-F+T(dF/dT)

"Normalized difference of the potential minima"

- β is defined as $\beta \equiv \left.\frac{1}{\Gamma}\frac{d\Gamma}{dt}\right|_{t=t_t}$ $\tilde{\beta}\left(\equiv \frac{\beta}{H_t}\right) = T_t \left.\frac{d(S_3(T)/T)}{dT}\right|_{T=T_t}$

"~How fast the minimum goes down"

GWs from 1stOPT

C. Caprini *et al.*, JCAP**1604**, 001 (2016)

Expanding
bubbles of the broken phase

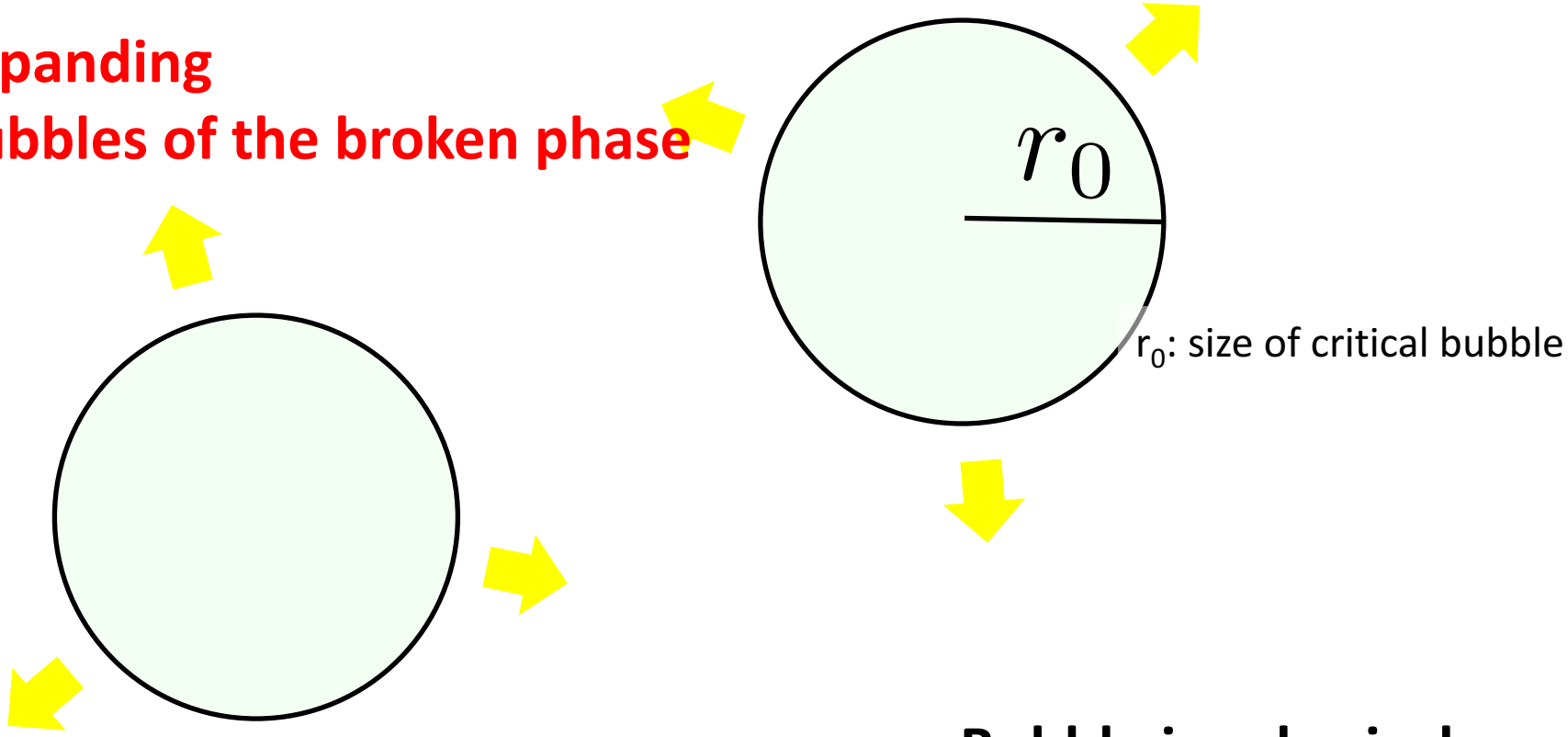

r_0: size of critical bubble

Bubble is spherical

No GW occurs

GWs from 1stOPT

C. Caprini *et al.*, JCAP**1604**, 001 (2016)

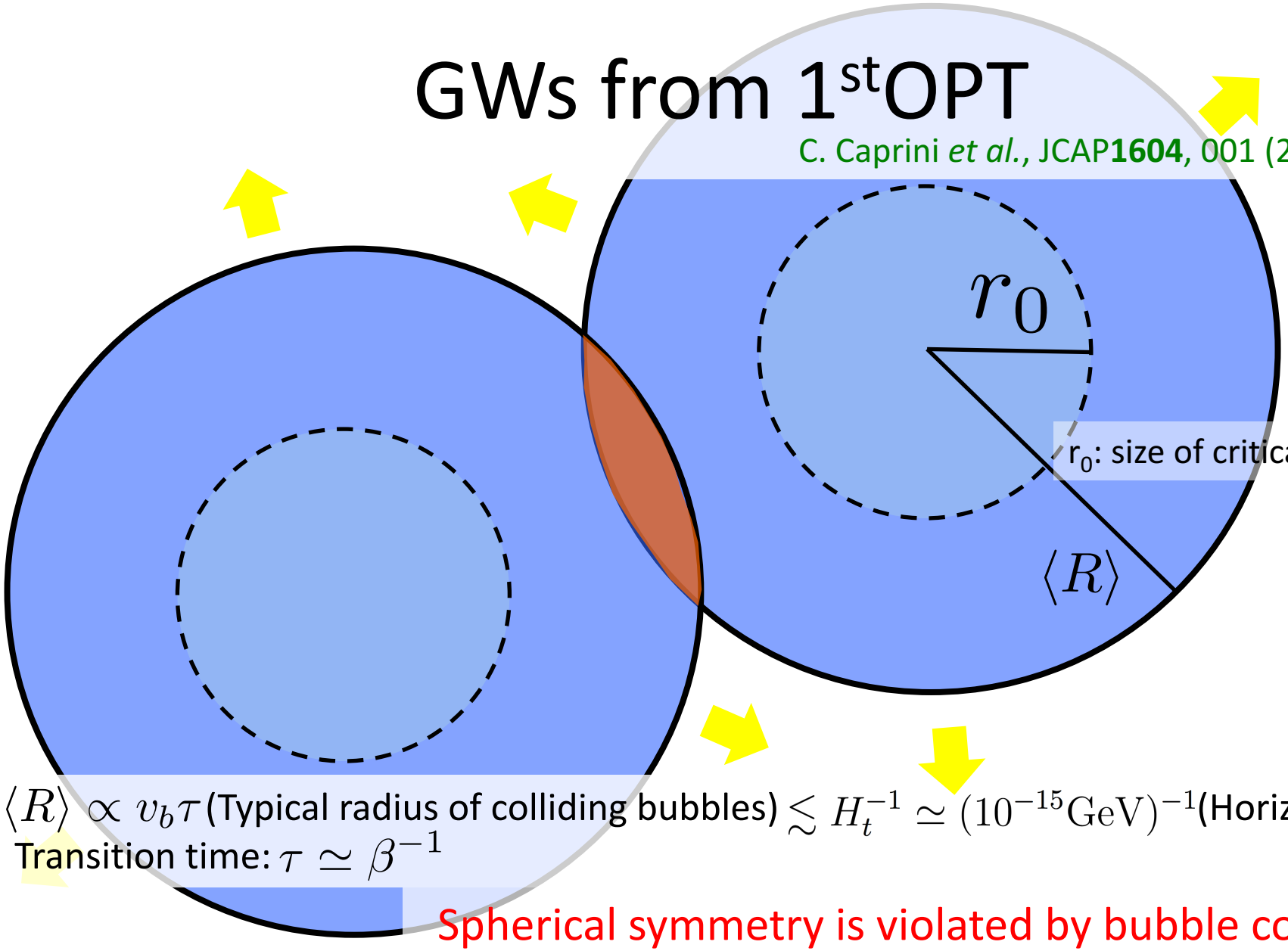

r_0: size of critical bubble

$\langle R \rangle \propto v_b \tau$ (Typical radius of colliding bubbles) $\lesssim H_t^{-1} \simeq (10^{-15}\mathrm{GeV})^{-1}$ (Horizon size),

Transition time: $\tau \simeq \beta^{-1}$

Spherical symmetry is violated by bubble collisions

GWs from 1stOPT

C. Caprini *et al.*, JCAP**1604**, 001 (2016)

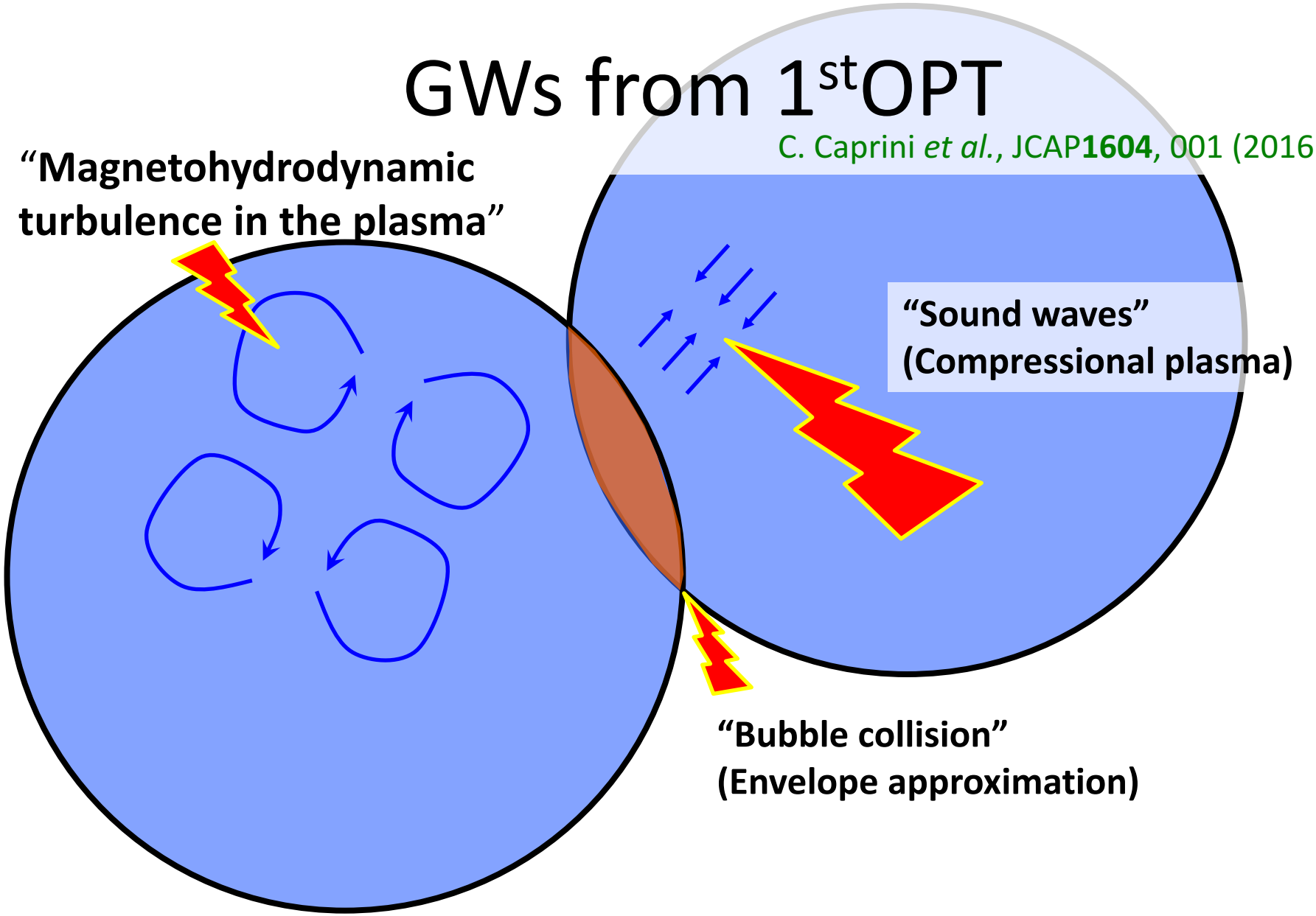

Relic abundance of GWs

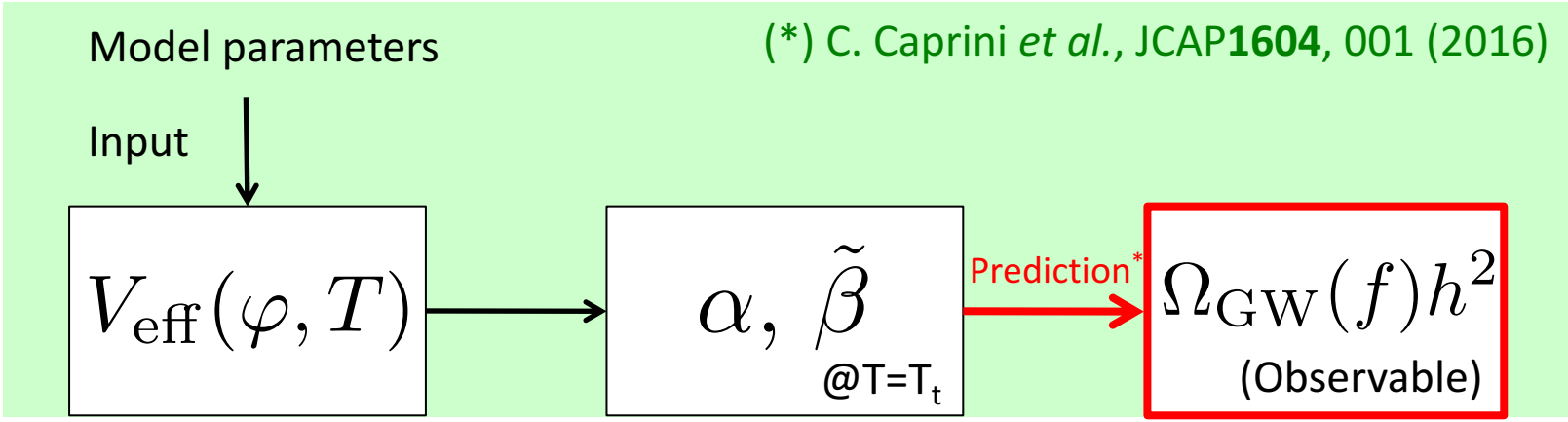

Relic abundance of GWs @ peak frequency

$$\widetilde{\Omega}_{\rm sw}h^2 \simeq 2.65\times10^{-6}\frac{v_b}{\tilde{\beta}}\left(\frac{\kappa(v_b,\alpha)\alpha}{1+\alpha}\right)^2 \quad @\ \tilde{f}_{\rm sw}\simeq 1.9\times10^{-5}\ {\rm Hz}\frac{\tilde{\beta}(T_t/100\ {\rm GeV})}{v_b}$$

$$\widetilde{\Omega}_{\rm env}h^2 \simeq \frac{1.84\times10^{-6}v_b^3}{(0.42+v_b^2)\tilde{\beta}^2}\left(\frac{\kappa(v_b,\alpha)\alpha}{1+\alpha}\right)^2 \quad @\ \tilde{f}_{\rm env}\simeq 1.0\times10^{-5}\ {\rm Hz}\frac{\tilde{\beta}(T_t/100\ {\rm GeV})}{1.8-0.1v_b+v_b^2}$$

$$\widetilde{\Omega}_{\rm turb}h^2 \simeq \frac{9.35\times10^{-8}v_b^2}{0.00354v_b\tilde{\beta}+\tilde{\beta}^2}\left(\frac{\epsilon\kappa(v_b,\alpha)\alpha}{1+\alpha}\right)^{3/2} \quad @\ \tilde{f}_{\rm turb}\simeq 2.7\times10^{-5}\ {\rm Hz}\frac{\tilde{\beta}(T_t/100\ {\rm GeV})}{v_b}$$

Estimation of the relic abundance

M. Kamionkowski, PRD**49**, 2837 (1994)

- Wave eq. from Einstein eq. in weak field approximation
- Stochastic backgrounds of GWs

$$-\Box\left(h_{\mu\nu}-\frac{1}{2}\eta_{\mu\nu}h^{\alpha}{}_{\alpha}\right)=16\pi G T_{\mu\nu}$$

$$\begin{cases} T^0_0=\rho_{\rm kin}+\cdots \\ \dfrac{d}{dt}\simeq\beta \end{cases}$$

$$\rho_{\rm GW}=\frac{1}{32\pi G}<\dot{h}_{\alpha\beta}\dot{h}^{\alpha\beta}>\sim 8\pi G\rho^2_{\rm kin}/\beta^2$$

$$\rho_{\rm tot}\left(=\underbrace{\rho_{\rm vac}}_{(=\epsilon)}+\rho_{\rm rad}\right)=\frac{3H^2}{8\pi G}$$

$$\alpha=\frac{\rho_{\rm vac}}{\rho_{\rm rad}}\qquad \kappa=\frac{\rho_{\rm vac}}{\rho_{\rm vac}}$$

Efficiency factor

$$\Omega_{\rm GW}=\frac{\rho_{GW}}{\rho_{\rm tot}}\simeq\underbrace{\left(\frac{H}{\beta}\right)^2}_{=\widetilde{\beta}^{-2}\sim(H\langle R\rangle)^2}\left(\frac{\kappa\alpha}{1+\alpha}\right)^2$$

Origins of GWs from EWPT

C. Caprini *et al.*, arXiv:1512.06239 [astro-ph.CO] (review)

2.1 Contributions to the Gravitational Wave Spectrum

To varying degrees, three processes are involved in the production of GWs at a first-order PT:

- Collisions of bubble walls and (where relevant) shocks in the plasma. This can be treated by a technique now generally referred to as the 'envelope approximation' [10–15]. As described below, this approximation can be used to compute the contribution to the GW spectrum from the scalar field, ϕ, itself.
- Sound waves in the plasma after the bubbles have collided but before expansion has dissipated the kinetic energy in the plasma [16–19].
- Magnetohydrodynamic (MHD) turbulence in the plasma forming after the bubbles have collided [20–25].

We improve our analysis in accordance with the recent simulation result.

Recent work of other souse of GW "sound wave"

M. Hindmarsh, *et al*., PRL **112**, 041301 (2014); arXiv:1504.03291 [astro-ph.CO].

Numerical simulations of acoustically generated gravitational waves at a first order phase transition

Mark Hindmarsh,[1,2,*] Stephan J. Huber,[1,†] Kari Rummukainen,[2,‡] and David J. Weir[3,§]

[1] *Department of Physics and Astronomy, University of Sussex, Falmer, Brighton BN1 9QH, U.K.*
[2] *Department of Physics and Helsinki Institute of Physics, PL 64, FI-00014 University of Helsinki, Finland*
[3] *Institute of Mathematics and Natural Sciences, University of Stavanger, 4036 Stavanger, Norway*

(Dated: April 14, 2015)

We present details of numerical simulations of the gravitational radiation produced by a first order thermal phase transition in the early universe. We confirm that the dominant source of gravitational waves is sound waves generated by the expanding bubbles of the low-temperature phase. We demonstrate that the sound waves have a power spectrum with power-law form between the scales set by the average bubble separation (which sets the length scale of the fluid flow L_f) and the bubble wall width. The sound waves generate gravitational waves whose power spectrum also has a power-law form, at a rate proportional to L_f and the square of the fluid kinetic energy density. We identify a dimensionless parameter $\tilde{\Omega}_{GW}$ characterising the efficiency of this "acoustic" gravitational wave production whose value is $8\pi\tilde{\Omega}_{GW} \simeq 0.8 \pm 0.1$ across all our simulations. We compare the acoustic gravitational waves with the standard prediction from the envelope approximation. Not only is the power spectrum steeper (apart from an initial transient) but the gravitational wave energy density is generically two orders of magnitude or more larger.

Origins of GWs from EWPT

C. Caprini *et al.*, arXiv:1512.06239 [astro-ph.CO] (review)

- Vacuum bubble velocity v_b
- Efficiency factor $\kappa(v_b, \alpha)$

$$\widetilde{\Omega}_{\rm sw} h^2 \simeq 2.65 \times 10^{-6} \frac{v_b}{\tilde{\beta}} \left(\frac{\kappa(v_b,\alpha)\alpha}{1+\alpha} \right)^2 \quad @ \quad \tilde{f}_{\rm sw} \simeq 1.9 \times 10^{-5} {\rm Hz} \frac{\tilde{\beta}}{v_b}$$

$$\widetilde{\Omega}_{\rm env} h^2 \simeq \frac{1.84 \times 10^{-6} v_b^3}{(0.42 + v_b^2)\tilde{\beta}^2} \left(\frac{\kappa(v_b,\alpha)\alpha}{1+\alpha} \right)^2 \quad @ \quad \tilde{f}_{\rm env} \simeq 1.0 \times 10^{-5} {\rm Hz} \frac{\tilde{\beta}}{1.8 - 0.1 v_b + v_b^2}$$

$$\widetilde{\Omega}_{\rm turb} h^2 \simeq \frac{9.35 \times 10^{-8} v_b^2}{0.00354 v_b \tilde{\beta} + \tilde{\beta}^2} \left(\frac{\epsilon\kappa(v_b,\alpha)\alpha}{1+\alpha} \right)^{3/2} \quad @ \quad \tilde{f}_{\rm turn} \simeq 2.7 \times 10^{-5} {\rm Hz} \frac{\tilde{\beta}}{v_b}$$

Origins of GWs from EWPT

C. Caprini *et al.*, arXiv:1512.06239 [astro-ph.CO] (review)

- Vacuum bubble velocity v_b

- Efficiency factor $\kappa(v_b, \alpha)$

$$\kappa(v_b, \alpha) \simeq O(0.01 - 0.1)$$

J.R.Espinosa, *et al*, JCAP **1006**, 028 (2010)

$$\widetilde{\Omega}_{\rm sw} h^2 \simeq 2.65 \times 10^{-6} \frac{v_b}{\tilde{\beta}} \left(\frac{\kappa(v_b, \alpha)\alpha}{1+\alpha} \right)^2 \quad @ \quad \tilde{f}_{\rm sw} \simeq 1.9 \times 10^{-5} {\rm Hz} \frac{\tilde{\beta}}{v_b}$$

$$\widetilde{\Omega}_{\rm env} h^2 \simeq \frac{1.84 \times 10^{-6} v_b^3}{(0.42 + v_b^2)\tilde{\beta}^2} \left(\frac{\kappa(v_b, \alpha)\alpha}{1+\alpha} \right)^2 \quad @ \quad \tilde{f}_{\rm env} \simeq 1.0 \times 10^{-5} {\rm Hz} \frac{\tilde{\beta}}{1.8 - 0.1 v_b + v_b^2}$$

$$\widetilde{\Omega}_{\rm turb} h^2 \simeq \frac{9.35 \times 10^{-8} v_b^2}{0.00354 v_b \tilde{\beta} + \tilde{\beta}^2} \left(\frac{\kappa(v_b, \alpha)\alpha}{1+\alpha} \right)^{3/2} \quad @ \quad \tilde{f}_{\rm turn} \simeq 2.7 \times 10^{-5} {\rm Hz} \frac{\tilde{\beta}}{v_b}$$

Origins of GWs from EWPT

C. Caprini *et al.*, arXiv:1512.06239 [astro-ph.CO] (review)

- Vacuum bubble velocity v_b
- Efficiency factor $\kappa(v_b, \alpha)$

$$\kappa(v_b, \alpha) \simeq O(0.01 - 0.1)$$

J.R.Espinosa, *et al*, JCAP **1006**, 028 (2010)

- The fraction of bulk motion from the bubble walls

The result from resent simulation

$$\epsilon \simeq 0.05 - 0.10$$

Hindmarsh, Huber, Rummukainen, Weir, PRD **92**, no. 12, 123009 (2015)

$$\widetilde{\Omega}_{\rm sw} h^2 \simeq 2.65 \times 10^{-6} \frac{v_b}{\tilde{\beta}} \left(\frac{\kappa(v_b, \alpha)\alpha}{1+\alpha} \right)^2 \quad @ \ \tilde{f}_{\rm sw} \simeq 1.9 \times 10^{-5} {\rm Hz} \frac{\tilde{\beta}}{v_b}$$

$$\widetilde{\Omega}_{\rm env} h^2 \simeq \frac{1.84 \times 10^{-6} v_b^3}{(0.42 + v_b^2)\tilde{\beta}^2} \left(\frac{\kappa(v_b, \alpha)\alpha}{1+\alpha} \right)^2 \quad @ \ \tilde{f}_{\rm env} \simeq 1.0 \times 10^{-5} {\rm Hz} \frac{\tilde{\beta}}{1.8 - 0.1 v_b + v_b^2}$$

$$\widetilde{\Omega}_{\rm turb} h^2 \simeq \frac{9.35 \times 10^{-8} v_b^2}{0.00354 v_b \tilde{\beta} + \tilde{\beta}^2} \left(\frac{\epsilon \kappa(v_b, \alpha)\alpha}{1+\alpha} \right)^{3/2} \quad @ \ \tilde{f}_{\rm turn} \simeq 2.7 \times 10^{-5} {\rm Hz} \frac{\tilde{\beta}}{v_b}$$

$(\alpha, \beta\text{tilde}) \Leftrightarrow (f, \Omega_{GW}h^2)_{new}$

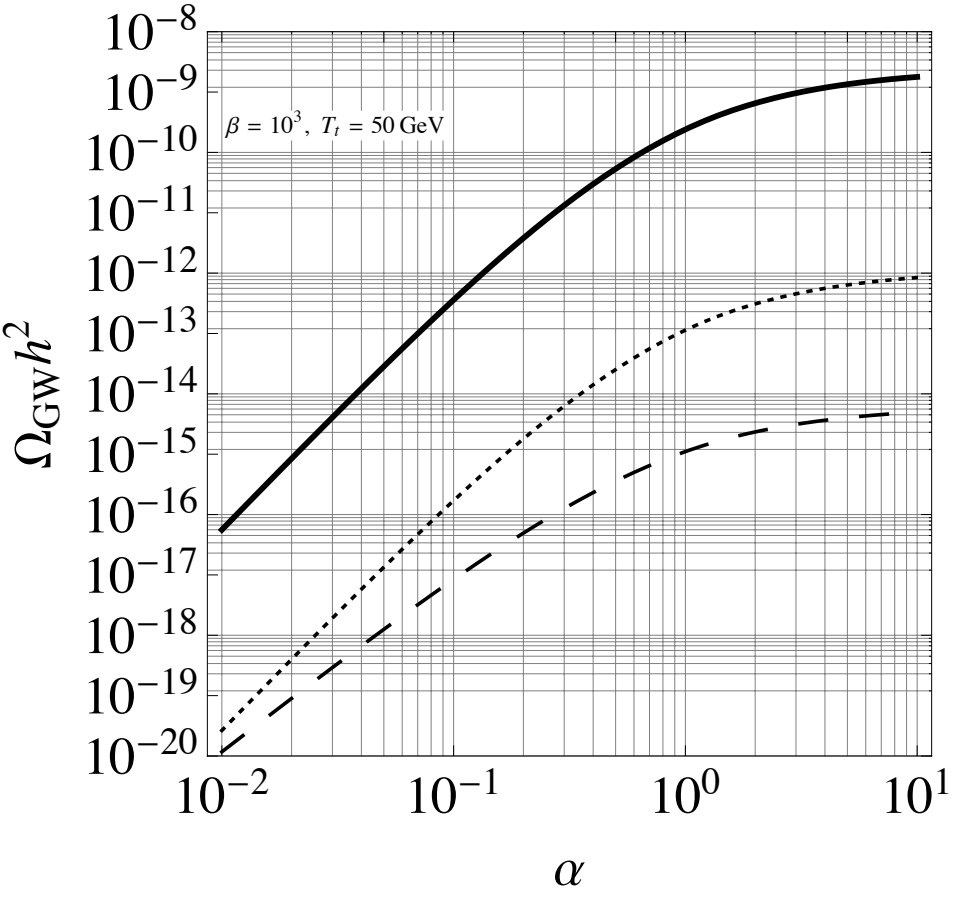

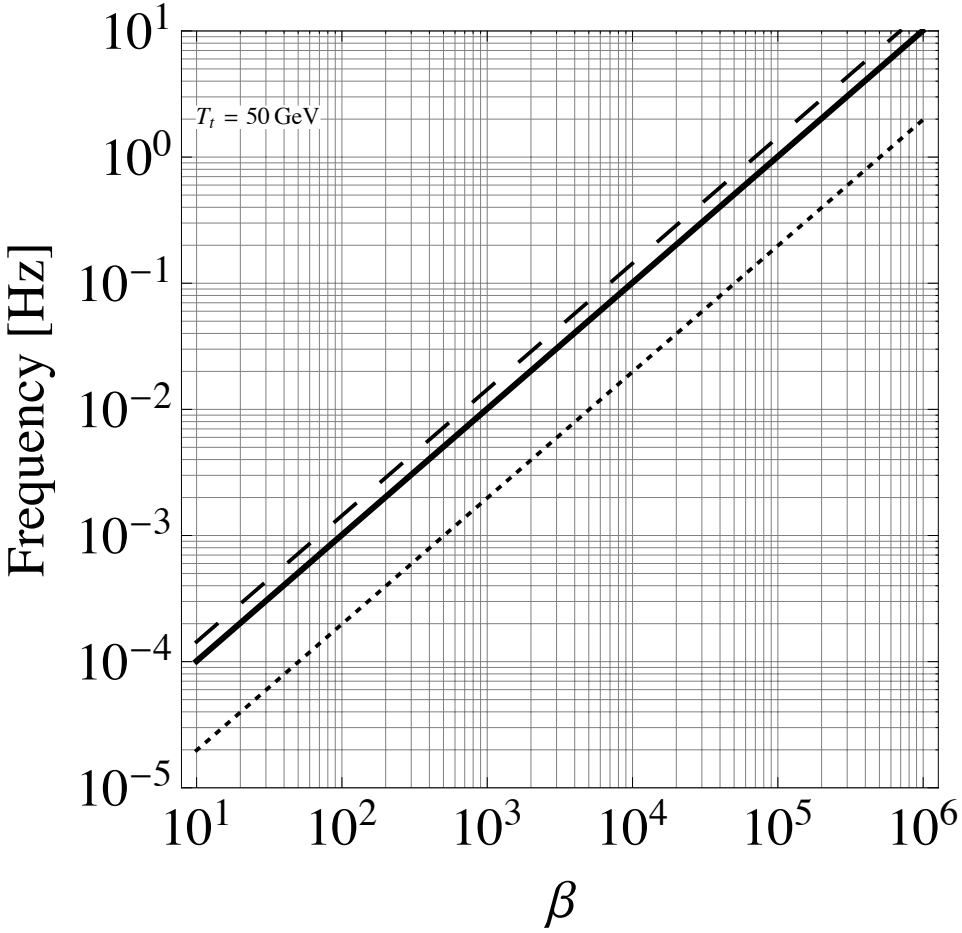

(α, βtilde)_exp. by New spectra (T_t=50GeV)

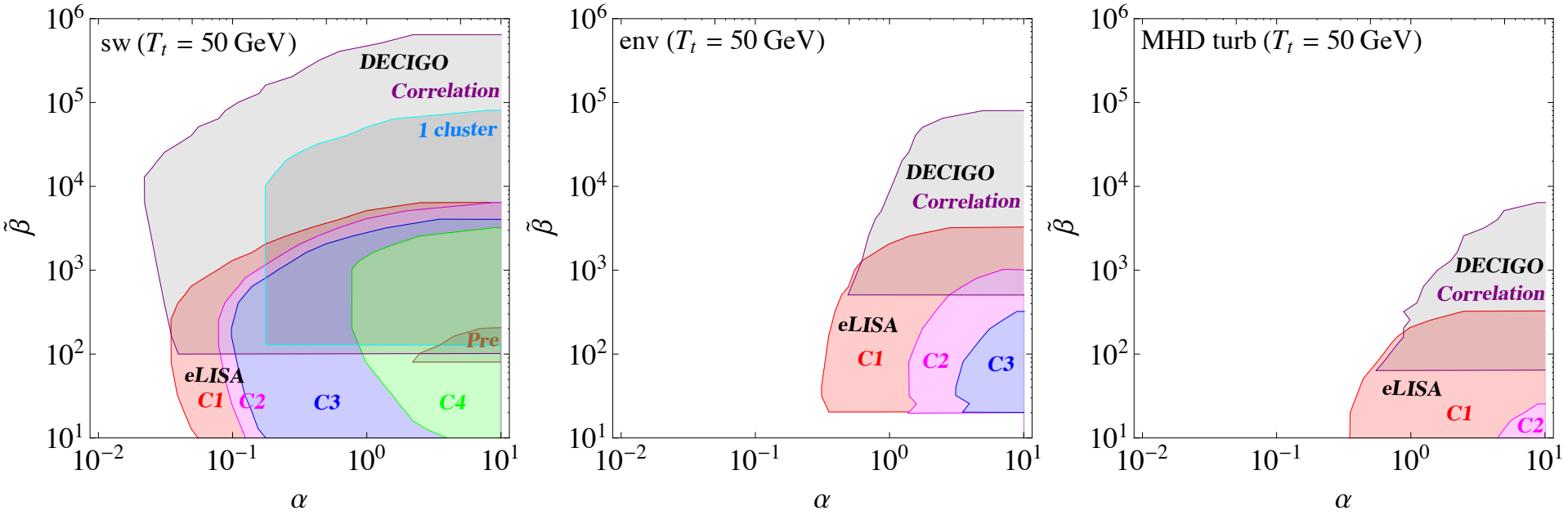

(α, βtilde)_exp. by New spectra (T_t=100GeV)

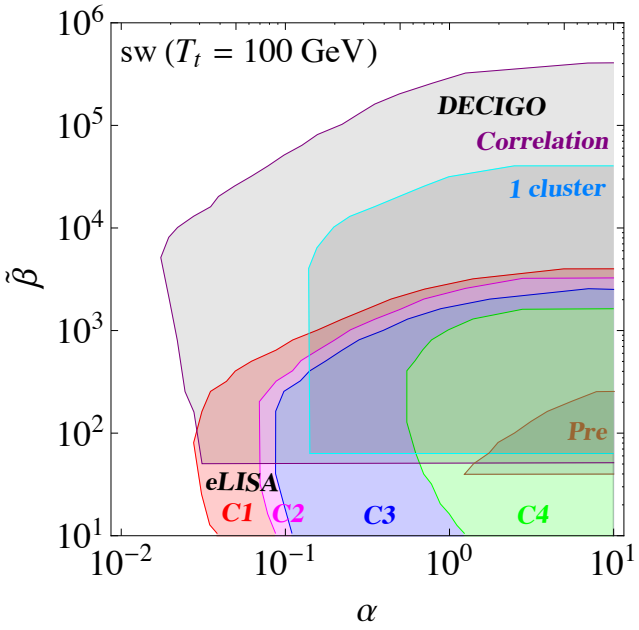

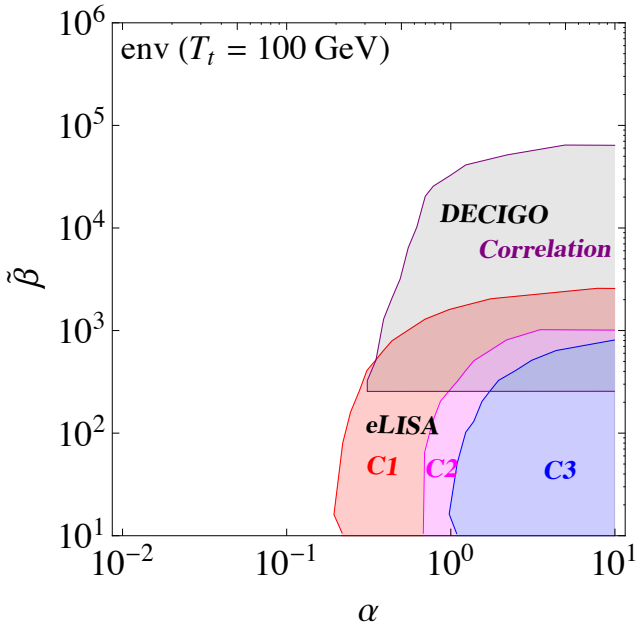

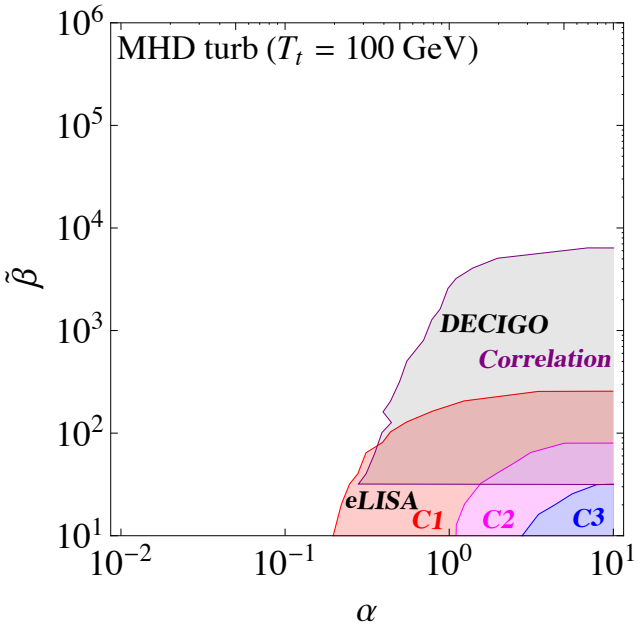

Efficiency factor $\kappa(v_b, \alpha)$

J. R. Espinosa, *et al*, JCAP **1006**, 028 (2010)

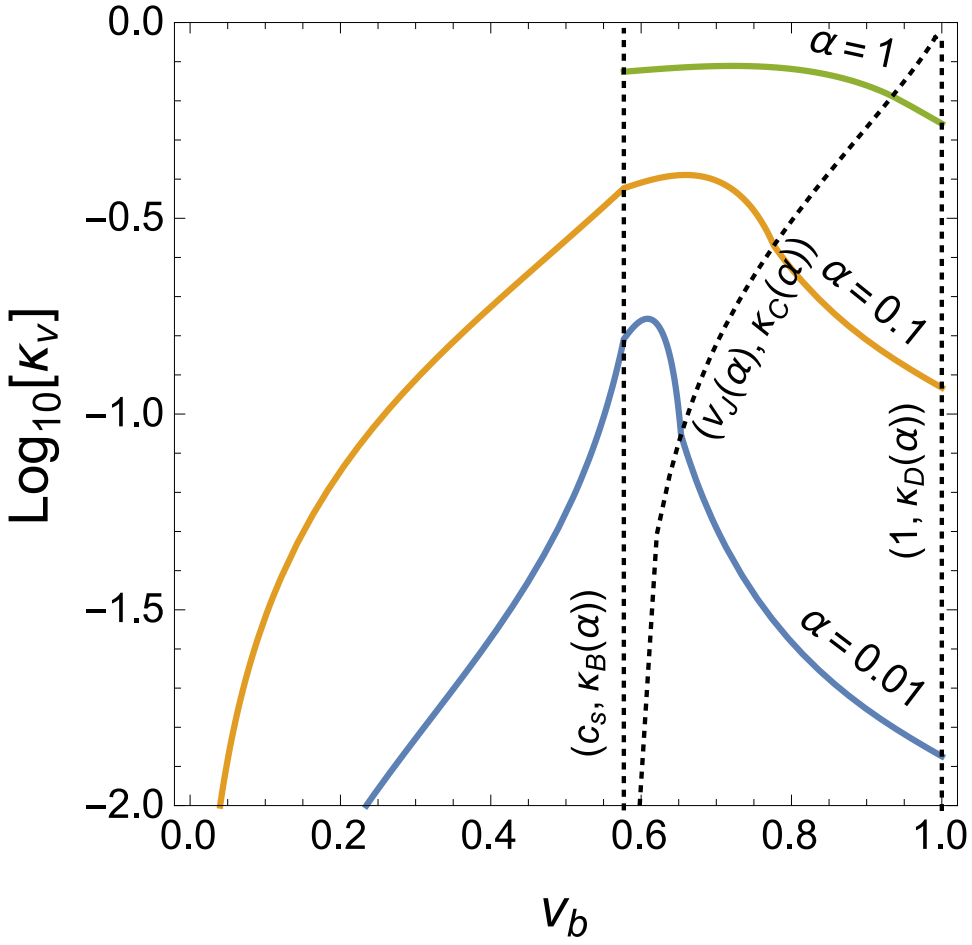

A Numerical fits to the efficiency coefficients J. R. Espinosa, *et al.*

In this section we provide fits to the numerical results of section 4. These fits facilitate the functions $\kappa(\xi_w, \alpha_N)$ and $\alpha_+(\xi_w, \alpha_N)$ without solving the flow equations and with a precision better that 15% in the region $10^{-3} < \alpha_N < 10$.

In order to fit the function $\kappa(\xi_w, \alpha_N)$, we split the parameter space into three regions and provide approximations for the four boundary cases and three families of functions that interpolate in-between: For small wall velocities one obtains ($\xi_w \ll c_s$)

$$\kappa_A \simeq \xi_w^{6/5} \frac{6.9\alpha_N}{1.36 - 0.037\sqrt{\alpha_N} + \alpha_N} \,. \tag{A.1}$$

For the transition from subsonic to supersonic deflagrations ($\xi_w = c_s$)

$$\kappa_B \simeq \frac{\alpha_N^{2/5}}{0.017 + (0.997 + \alpha_N)^{2/5}} \,. \tag{A.2}$$

ξ_J is same as our $v_b(\alpha)$

For Jouguet detonations ($\xi_w = \xi_J$), as stated in eq. (4.2)

$$\kappa_C \simeq \frac{\sqrt{\alpha_N}}{0.135 + \sqrt{0.98 + \alpha_N}} \quad \text{and} \quad \xi_J = \frac{\sqrt{\frac{2}{3}\alpha_N + \alpha_N^2} + \sqrt{1/3}}{1 + \alpha_N} \,. \tag{A.3}$$

And finally for very large wall velocity, ($\xi_w \to 1$) as stated in eq. (4.4)

$$\kappa_D \simeq \frac{\alpha_N}{0.73 + 0.083\sqrt{\alpha_N} + \alpha_N} \,. \tag{A.4}$$

For subsonic deflagrations a good fit to the numerical results is provided by

$$\kappa(\xi_w \lesssim c_s) \simeq \frac{c_s^{11/5} \kappa_A \kappa_B}{(c_s^{11/5} - \xi_w^{11/5})\kappa_B + \xi_w c_s^{6/5} \kappa_A} \,, \tag{A.5}$$

and for detonations by

$$\kappa(\xi_w \gtrsim \xi_J) \simeq \frac{(\xi_J - 1)^3 \xi_J^{5/2} \xi_w^{-5/2} \kappa_C \kappa_D}{[(\xi_J - 1)^3 - (\xi_w - 1)^3]\xi_J^{5/2} \kappa_C + (\xi_w - 1)^3 \kappa_D} \,. \tag{A.6}$$

The numerical result for the hybrid (supersonic deflagration) region is well described by a cubic polynomial. As boundary conditions, one best uses the two values of κ and the first derivative of κ at $\xi_w = c_s$. Notice that the derivative of κ in ξ_w is not continuous at the point ξ_J. The derivative at $\xi_w = c_s$ is approximately given by

$$\delta\kappa \simeq -0.9 \log \frac{\sqrt{\alpha_N}}{1 + \sqrt{\alpha_N}} \,. \tag{A.7}$$

This differs from the derivative one would obtain from the fit in the region $\xi_w < c_s$, but mostly for values $\alpha \gtrsim 1$, where no solutions exist for $\xi_w < c_s$. The expression for supersonic deflagrations then reads

$$\kappa(c_s < \xi_w < \xi_J) \simeq \kappa_B + (\xi_w - c_s)\delta\kappa + \frac{(\xi_w - c_s)^3}{(\xi_J - c_s)^3}[\kappa_C - \kappa_B - (\xi_J - c_s)\delta\kappa] \,. \tag{A.8}$$

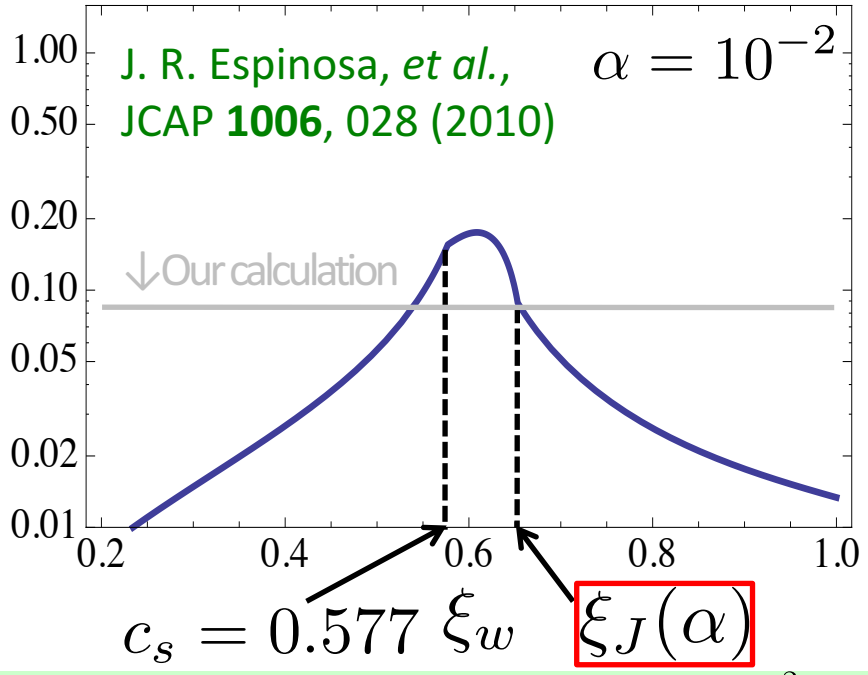

$$\widetilde{\Omega}_{\rm coll} h^2 \simeq \frac{1.8 \times 10^{-6} (\kappa(\alpha, \xi_w))^2 \xi_w^3}{0.42 + \xi_w^2} \times \left(\frac{\alpha}{1+\alpha}\right)^2 \tilde{\beta}^{-2}$$

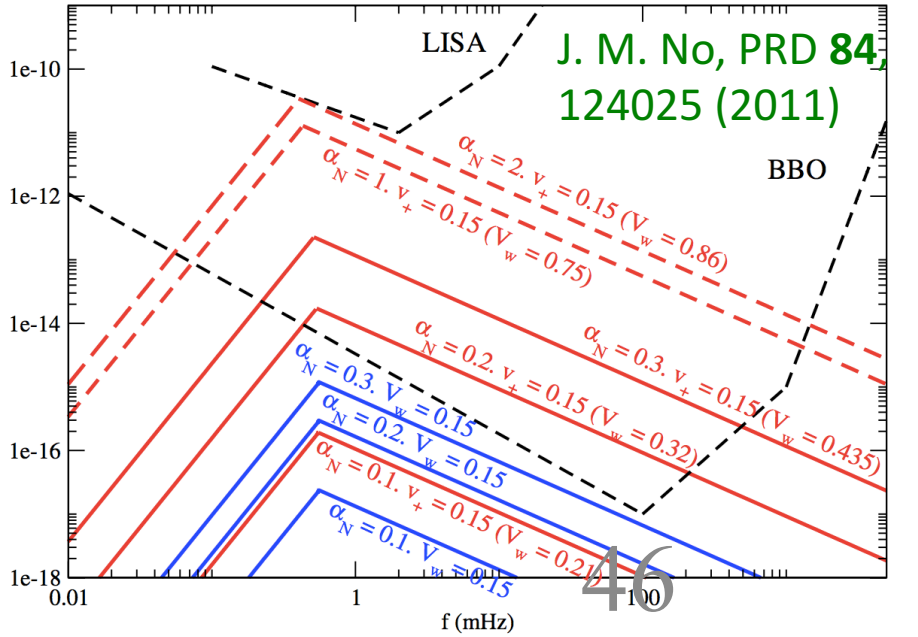

Contour plot of α on (ξ_w, v_+) plane

α is given by effective potential.

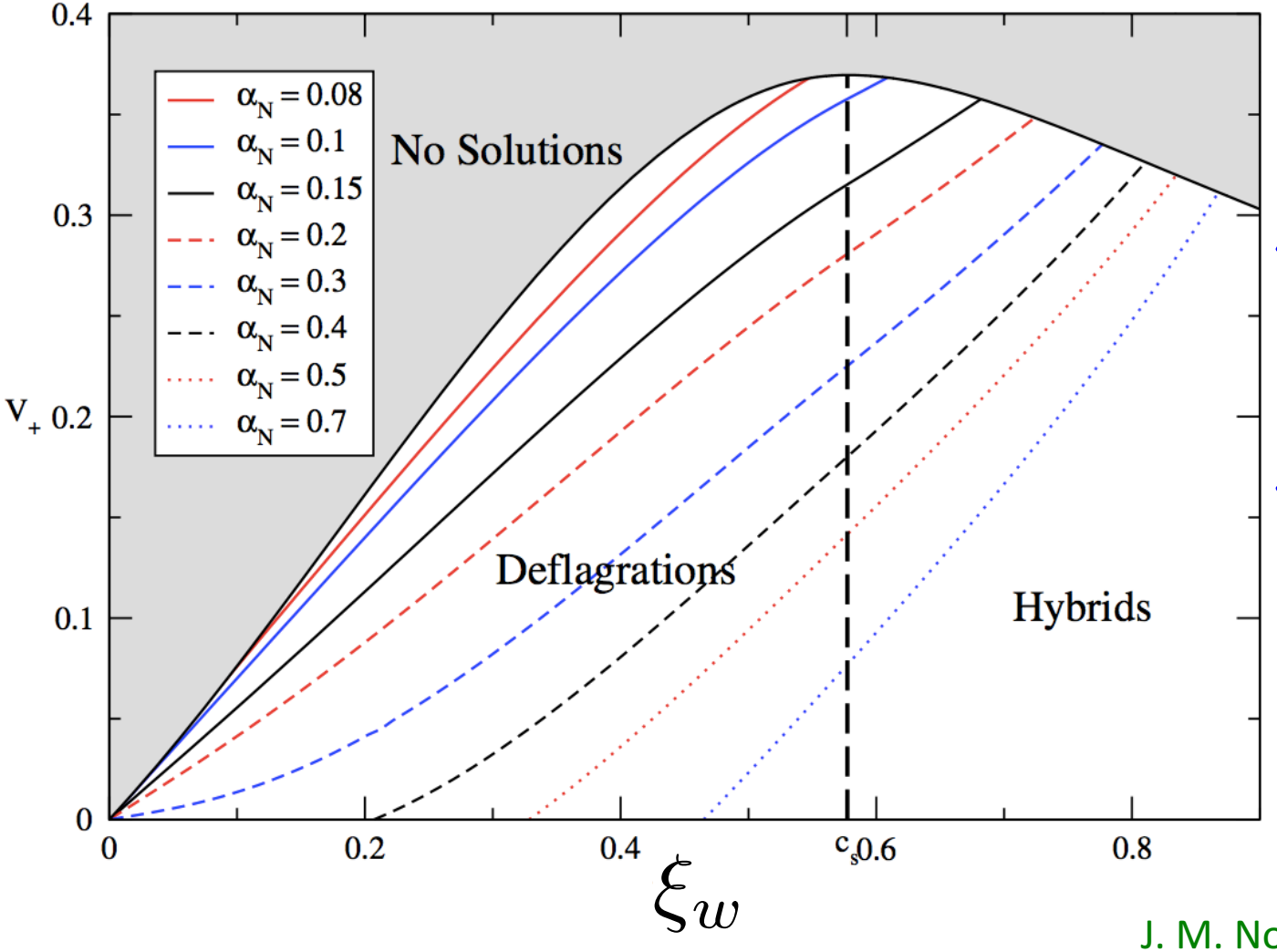

Diffusion upper bound of EWBG

EWBG requires small ξ_w
⇎GW requires large

J. M. No, PRD84, 124025 (2011)

Contour plot of v_+ on (ξ_w, α) plane

α is given by effective potential.

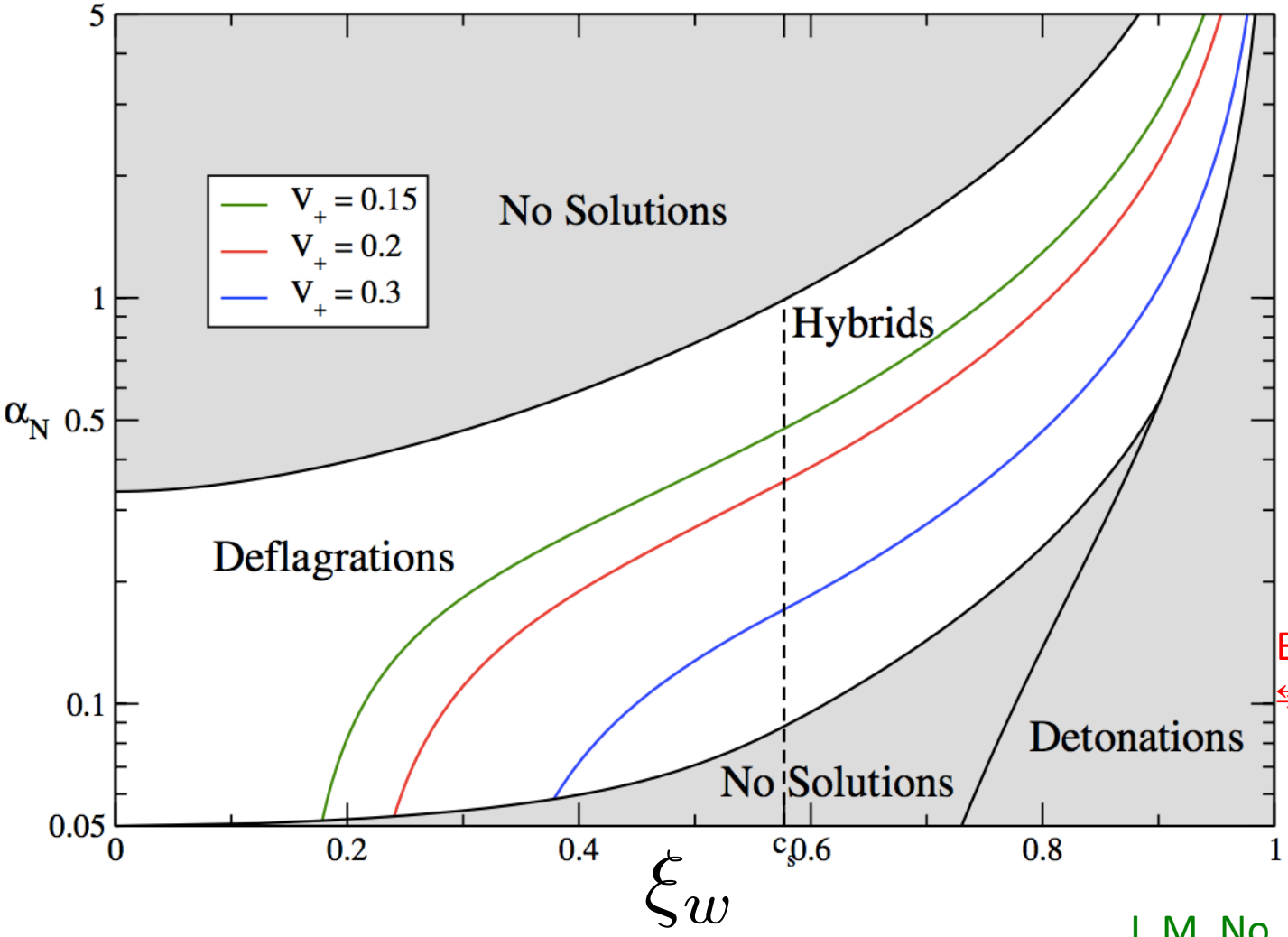

EWBG requires small ξ_w
⇎GW requires large

J. M. No, PRD84, 124025 (2011)

Foreground noise from white dwarf binaries

R. Schneider, S. Marassi, V. Ferrari, Class. Quant. Grav. **27**, 194007 (2010)

Stochastic backgrounds of gravitational waves from extragalactic sources

R Schneider[1], S Marassi[2], V Ferrari[2]

[1] INAF, Osservatorio Astrofisico di Arcetri, Largo Enrico Fermi 5, 50125, Firenze, Italy

[2] Dipartimento di Fisica G.Marconi, Sapienza Universit'a di Roma and Sezione INFN ROMA1, piazzale Aldo Moro 2, I-00185 Roma, Italy

E-mail: raffa@arcetri.astro.it

Abstract.

Astrophysical sources emit gravitational waves in a large variety of processes occurred since the beginning of star and galaxy formation. These waves permeate our high redshift Universe, and form a background which is the result of the superposition of different components, each associated to a specific astrophysical process. Each component has different spectral properties and features that it is important to investigate in view of a possible, future detection. In this contribution, we will review recent theoretical predictions for backgrounds produced by extragalactic sources and discuss their detectability with current and future gravitational wave observatories.

Gravitational wave Models

Strongly 1st order phase transition

～ Mechanisms to create the potential barrier～

- Non-thermal tree level effects (−*e*)

Analytic formula (High temperature approximation)

$$\frac{\varphi_c}{T_c} = \frac{2E}{\lambda}\left(1 - \frac{e\lambda}{ET}\right)$$

$$V_{\rm eff} = D(T^2 - T_0^2)\varphi^2 - (ET - e)\varphi^3 + \frac{\lambda(T)}{4}\varphi^4$$

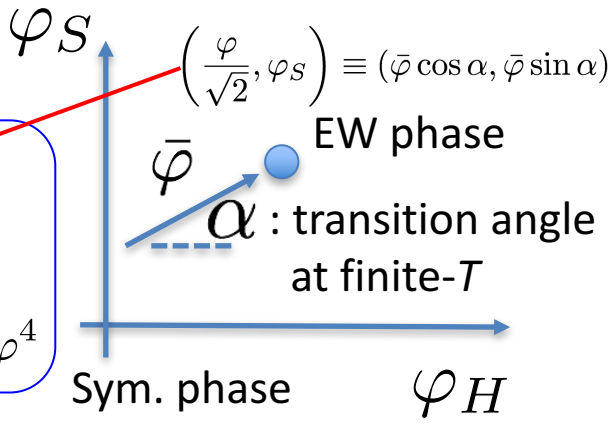

e.g. Higgs singlet model (HSM)

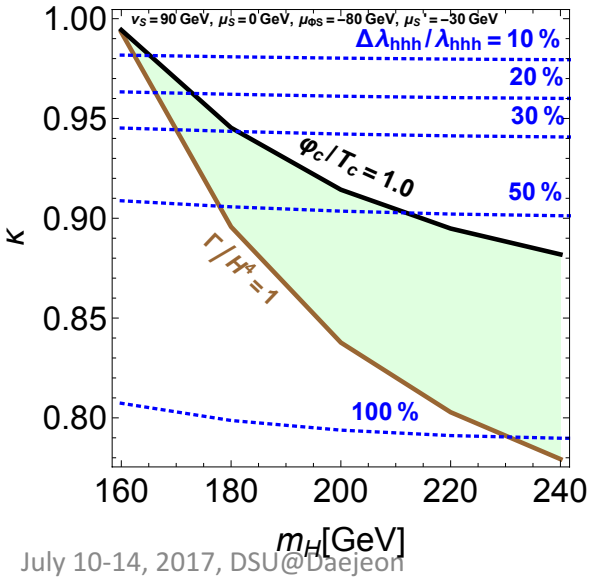

$$V_0 = -\mu_\Phi^2|\Phi|^2 + \lambda_\Phi|\Phi|^4 + \mu_{\Phi S}|\Phi|^2 S + \frac{\lambda_{\Phi S}}{2}|\Phi|^2 S^2 + \mu_S^3 S + \frac{m_S^2}{2}S^2 + \frac{\mu_S'}{3}S^3 + \frac{\lambda_S}{4}S^4$$

$$e = \left(\mu_{\Phi S}\cos^2\alpha + \frac{\mu_S'}{3}\sin^2\alpha\right)\sin\alpha \quad <0$$

$$\frac{\Delta\lambda_{hhh}}{\lambda_{hhh}} \equiv \frac{\lambda_{hhh} - \lambda_{hhh}^{\rm SM}}{\lambda_{hhh}^{\rm SM}}$$

θ : mixing angle at zero-T

$$\lambda_{hhh}^{\rm HSM,tree} = 6\left(\lambda_\Phi v_\Phi c_\theta^3 + \frac{\mu_{\Phi S}}{2}s_\theta c_\theta^2 + \frac{\lambda_{\Phi S}}{2}s_\theta c_\theta(v_\Phi s_\theta + v_S c_\theta) + \left(\frac{\mu_S'}{3} + \lambda_S v_S\right)s_\theta^3\right)$$

$$\kappa_i \equiv g_{hii}/g_{hii}^{\rm SM}$$

$$\kappa \equiv \kappa_V = \kappa_F = \cos\theta$$

Fuyuto, Senaha, PRD **90**, no. 1, 015015 (2014)
Hashino, Kakizaki, Kanemura, TM, Ko, PLB **766**, 49 (2017)

Multi-field analysis of EWPT

K. Funakubo, S. Tao and F. Toyoda, Prog. Theor. Phys. 114, 369 (2005) (NMSSM)
K. Fuyuto and E. Senaha, Phys. Rev. D 90, no. 1, 015015 (2014) (HSM)

- EWPT:

$$(\varphi_\Phi, \varphi_S)_{\rm SYM} \to (\varphi_\Phi, \varphi_S)_{\rm EW} \quad @T=T_c,\ \varphi_c \equiv \varphi_\Phi(T_c)$$

- Diverse patterns of the EWPT:

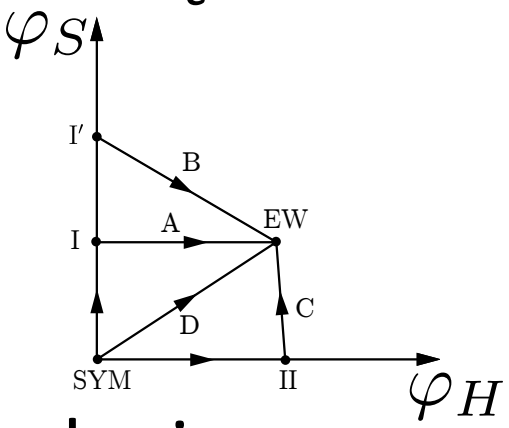

- EW phase needs to be the global min.:

$$V_{{\rm eff},T=0}(\text{EW phase}) < V_{{\rm eff},T=0}(\text{other phases})$$

- Public tool “CosmoTransition” (Python code) is used.

Theoretical constraints

- Perturbative unitarity: $|a_0(W_L^+ W_L^- \to W_L^+ W_L^-)| \leq 1$

$$m_h^2 \cos^2\theta + m_H^2 \sin^2\theta \leq \frac{4\pi\sqrt{2}}{3G_F} \approx (700\mathrm{GeV})^2$$

- Vacuum stability:

$$\lambda_\Phi(\mu) > 0, \qquad \lambda_S(\mu) > 0, \qquad 4\lambda_\Phi(\mu)\lambda_S(\mu) > \lambda_{\Phi S}^2(\mu)$$

- Landau pole:

$$|\lambda_{\Phi,S,\Phi S}(\Lambda_{\mathrm{LP}})| = 4\pi$$

- Oblique parameters (*S*, *T*, *U*):

$$\cos\theta \gtrsim 0.92 \quad \text{when } m_H \gtrsim 400\mathrm{GeV}\ (m_h \approx 125\mathrm{GeV})$$

S. Baek, P. Ko, W. I. Park and E. Senaha, JHEP 1211, 116 (2012)

Singlet extension of the SM (non-thermal)

A. Ashoorioon, T. Konstandin, JCAP**0809**, 022 (2008)

- Potential $S = s + x$

$$V_0(\Phi, S) = V_{\rm SM}(\Phi) + b_1 S + \frac{b_2}{2} S^2 + \frac{b_3}{3} S^3 + \frac{b_4}{4} S^4 + \frac{a_1}{2} |\Phi|^2 S + \frac{a_2}{2} |\Phi|^2 S^2$$

- An example of the paths (assumption)

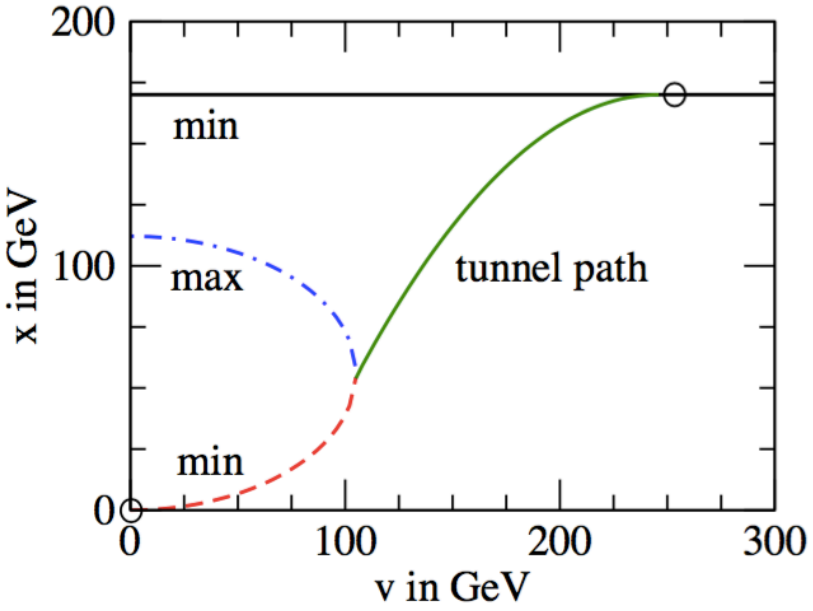

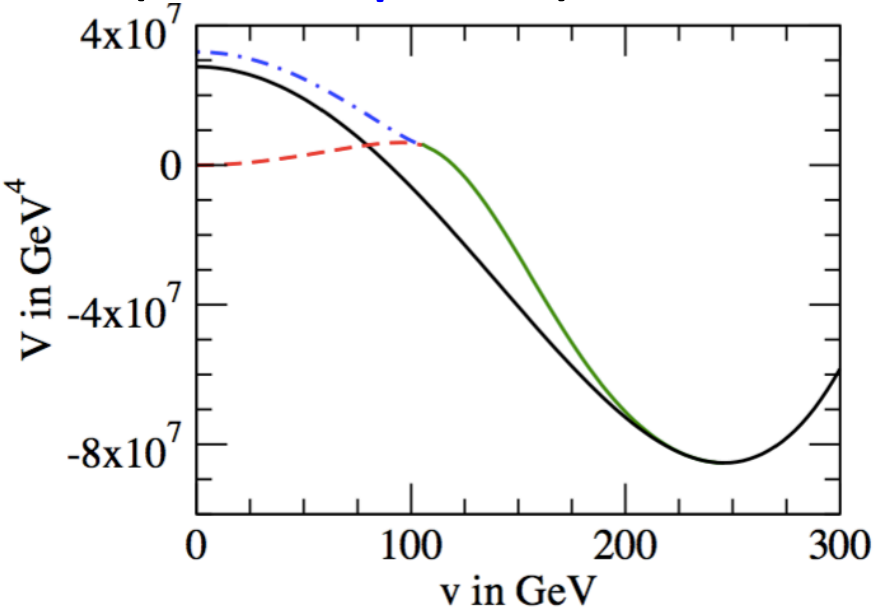

Singlet extension of the SM (non-thermal)

A. Ashoorioon, T. Konstandin, JCAP**0809**, 022 (2008)

$\bar{\mu}_s$/ GeV	α	β/H	v/T	T / GeV
190	0.14	121	3.1	75
186	0.18	88	3.4	69
183	0.25	53	3.7	63
181	0.33	25	4.0	57
180	0.42	8	4.2	54
179	symmetric phase stable			

Results(↑,→)

$$\bar{\mu}_h^2 = \left.\frac{\partial^2 V}{\partial v^2}\right|_{v=\bar{v},\, x=\bar{x}}, \quad \bar{\mu}_s^2 = \left.\frac{\partial^2 V}{\partial x^2}\right|_{v=\bar{v},\, x=\bar{x}}, \quad \bar{\mu}_{hs}^2 = \left.\frac{\partial^2 V}{\partial v \partial x}\right|_{v=\bar{v},\, x=\bar{x}}$$